**ISTANBUL TECHNICAL UNIVERSITY ★ GRADUATE SCHOOL OF SCIENCE ENGINEERING AND TECHNOLOGY**

# A STUDY ON THE EFFECT OF PRESSURE ON IN SITU COMBUSTION KINETICS OF BATI RAMAN CRUDE BY CONVENTIONAL AND ISOCONVENTIONAL METHODS

**M.Sc. THESIS**
**EVANS ANTO – DARKWAH**

**Department of Petroleum and Natural Gas Engineering**

**Petroleum and Natural Gas Engineering Programme**

**DECEMBER 2015**

**ISTANBUL TECHNICAL UNIVERSITY ★ GRADUATE SCHOOL OF SCIENCE ENGINEERING AND TECHNOLOGY**

# A STUDY ON THE EFFECT OF PRESSURE ON IN SITU COMBUSTION KINETICS OF BATI RAMAN CRUDE BY CONVENTIONAL AND ISOCONVENTIONAL METHODS

**M.Sc. THESIS**
**EVANS ANTO – DARKWAH**
**(505121502)**

**Department of Petroleum and Natural Gas Engineering**

**Petroleum and Natural Gas Engineering Programme**

**Thesis Advisor: Assistant Prof. Dr. MURAT ÇINAR**

**DECEMBER 2015**

**İSTANBUL TEKNİK ÜNİVERSİTESİ ★ FEN BİLİMLERİ ENSTİTÜSÜ**

# BATI RAMAN PETROLÜNÜN YERİNDE YANMA KİNETİĞİNE BASINCIN ETKİSİNİN ALIŞILAGELMİŞ VE EŞDÖNÜŞÜM YÖNTEMLERİ İLE İNCELENMESİ

**YÜKSEK LİSANS TEZİ**

**EVANS ANTO – DARKWAH**
**(505121502)**

**Petrol ve Doğal Gaz Mühendisliği Anabilim Dalı**

**Petrol ve Doğal Gaz Mühendisliği Programı**

**Tez Danışmanı: Yard. Doç. Dr. MURAT ÇINAR**

**ARALIK 2015**

**Evans Anto–Darkwah**, a **M.Sc.** student of ITU **Graduate School of Science Engineering and Technology** student ID **505121502**, successfully defended the **thesis** entitled **"A Study on the Effect of Pressure on In Situ Combustion Kinetics of Batı Raman Crude by Coventional and Isoconversional Methods "**, which he prepared after fulfilling the requirements specified in the associated legislations, before the jury whose signatures are below.

**Thesis Advisor :** **Asst. Prof. Murat Çınar .....**
Istanbul Technical University

**Jury Members :** **Prof. Mustafa Onur.....**
Istanbul Technical University

**Assoc. Prof. Nurgül Çelik Balcı.....**
Istanbul Technical University

**Date of Submission : 25 November 2015**
**Date of Defense : 16 December 2015**

***To my parents and siblings,***

**FOREWORD**

I would like to express my sincerest gratitude to Asst. Prof. Dr. Murat Çınar, who accepted me into his laboratory and also served as my thesis supervisor. I am deeply grateful for his comments, suggestions and corrections where it was required.

I also say thank you to Melek Deniz Parker and Eda Ay for their support in the In Situ Combustion Laboratory. I have benefited immensely from their great kindness, guidance and motivation accorded me during my laboratory sessions. I am grateful to all faculty members and fellow students in the Petroleum and Natural Gas Department for their immense help extended to me during my studies. For this I say a heartfelt thank you. To my beloved parents, Augustine Kwaku Anto and Margaret Awuah, I owe a deep debt of gratitude for their contributions to my life. My special thanks also goes to my siblings and uncle Philip Baffour-Awuah for their unflinchnig support and words of encouragement during the entire period of my studies. I am also grateful to Prof. Dr. Mustafa Onur and Assoc. Prof. Dr. Nurgül Çelik Balcı for accepting in a very quick time to serve on my jury.

Finally, I would like to thank the Governments of Ghana and Turkey for supporting the financial aspect of my education wholely without which life would have been very difficult.

December 2015 Evans Anto – Darkwah

**TABLE OF CONTENTS**

**Page**

**ABBREVIATIONS**

| | |
|---|---|
| **API** | **:**American Petroleum Institute |
| **DTA** | **:**Differential Thermal Analysis |
| **EGA** | **:**Effluent Gas Analysis |
| **EOR** | **:**Enhanced Oil Recovery |
| **HTO** | **:**High Temperature Oxidation |
| **ISC** | **:**In Situ Combustion |
| **LTO** | **:**Low Temperature Oxidation |
| **MTR** | **:**Middle Temperature Reactions |
| **NTGR** | **:**Negative Temperature Gradient Region |
| **OOIP** | **:**Original-Oil-In-Place |
| **RRR** | **:**Relative Reaction Rate |
| **RTO** | **:**Ramped Temperature Oxidation |
| **SARA** | **:**Saturates, Aromatics, Resins and Asphalthenes |
| **SLPM** | **:**Standard Liters Per Minute |
| **TGA** | **:**Thermogravimetric Analysis |
| **USGS** | **:**United States Geological Survey |

**SYMBOLS**

| | |
|---|---|
| **a** | **:**Reaction order (exponent) with respect to oxygen partial pressure in reaction rate equation |
| **A** | **:**Arrhenius constant in the Arrhenius reaction rate equation |
| **$A_c$** | **:**Cross - sectional area of the kinetic cell |
| **b** | **:**reaction order (exponent) with respect to carbon (fuel) concentration in reaction rate equation |
| **C** | **:**Concentration, mol/lt (mole %) |
| **$C_f$** | **:**Fuel concentration, mol/lt (mole %) |
| **CO** | **:**Carbon monoxide |
| **$CO_2$** | **:**Carbon dioxide |
| $\Delta C_{O_2}$ | **:**Change in concentration of oxygen, mol/lt (mole %) |
| **E** | **:**Activation energy, J/mol |
| ***f(X)*** | **:**Expression for concentration dependence on conversion |
| ***F*** | **:**Molar flow rate, mol/min |
| ***$F_{O_2}$*** | **:**Molar flow rate of oxygen, mol/min |
| **K(T)** | **:**Rate constant |
| **$O_2$** | **:**Oxygen |
| $P_{O_2}$ | **:**Partial pressure of oxygen, psig |
| **q** | **:**Volumetric flow rate, lt/min |
| **$r_{fuel}$ ($dC_{fuel}/dt$)** | **:**Rate of reaction with respect to carbon (fuel) |
| **R** | **:**Universal gas constant, $Jmol^{-1}K^{-1}$ |
| **t** | **:**Time, s |
| **T** | **:**Absolute temperature, K ($^oC$) |
| **X** | **:**Conversion |
| **v** | **:**Moles of oxygen that reacts with 1g of fuel in Fassihi's oxidation model |
| ***α*** | **:**Moles of oxygen consumed per mole of fuel that reacts in isoconversional equation |

**LIST OF TABLES**

**Page**

**LIST OF FIGURES**

**Page**

**A STUDY ON THE EFFECT OF PRESSURE ON IN SITU COMBUSTION KINETICS OF BATI RAMAN CRUDE BY CONVENTIONAL AND ISOCONVENTIONAL METHODS**

## SUMMARY

Crude oils are often grouped into three categories based on specific gravity range as either; heavy oil ($10^o$ – $20^o$ API), intermediate oil ($20^o$ – $30^o$ API), or light oils (> $30^o$ API). A fourth classification is the so-called extra heavy oils (<$10^o$). Heavy oils have higher viscosities (> 100 cp) and contain larger molecular weight components. Conventional oils (light oils) consist of only 30 % of the world oil resources and therefore technology and resources must be focused on how to extract the abundant heavy and bitumen resources in the various parts of the world.

Current methods for extracting heavy and bitumen resources are usually grouped as thermal and non-thermal methods. For very viscous oils, thermal methods, which employ the use of heat to reduce oil viscosity, are usually preferred. Thermal methods include, steam injection, in situ combustion, and hot water injection. On the other non-thermal methods of oil recovery such as waterflooding, $CO_2$ flooding etc. are employed for less viscous oils. Surface mining is usually employed in bitumen extraction, since there is practically no mobility in bitumen reservoirs and waterflooding is a preferred choice in North Sea area where heavy oils are less viscous. Steam injection, which is by far the most popular of the thermal methods, involves the use of an injection well to introduce steam into the reservoir and the use of a production well to produce the mobilized oil from the effect of the steam. The main problem with steam injection method is heat losses. Heat losses for steam injection occurs in the surface lines used for the transportation of steam, in the wellbore to the surrounding formations and in the reservior to overburden and underburden. In addition, problem of gravity override is experienced in relatively thicker formations. In situ combustion, which has been around for a while, is not as limited as steam injection. It is mainly applied as dry forward combustion, in which dry air is injected to a reservoir to create a hot air sweep within the reservoir, as wet forward combustion in which a water alternating gas process is employed to utilize the heat generated efficiently through the water vapor and the hot air sweep and finally as reverse combustion, where injected air and burning zones move counter currently. The main advantage of the in situ combustion process is the generation of heat in situ within the reservoir and the containment of combustion products within the reservoir. The air required for injection is free and can be found in any environment – onshore or offshore. The in situ combustion process is however complex and difficult to engineer and requires several laboratory studies to acquire kinetic parameters and to formulate appropriate reaction models to understand the burning characteristics of the oil involved during the combustion process.

The main objectives of this study is to formulate reaction models for the Bati Raman crude oil, a 12º API heavy oil from the Southeastern part of Turkey, to study pressure effect on the isoconversional kinetic analysis, and finally to predict the suitability of the crude oil to undergo combustion using isoconversional methods. Combustion kinetic studies within the literature usually fall under conventional and isoconversional methods. Conventional in situ combustion kinetic studies done by Tadema (1959), Bousaid and Ramey (1968) and Fassihi (1981) all apply a sort of straight-line approach in their interpretation of kinetic data. In these studies, reactions are grouped and lumped together but in reality, crude oil combustion involves several complex reactions. The isoconversional approach, however, provides model free methods which can by-pass the complex reaction model for activation energy estimation. The isoconversional method also provides screening criteria for determination of good and bad candidates for combustion. Conventional and isoconversional studies, which have been done previously point to three main reactions during in-situ combustion process. These reactions are namely: Low Temperature Oxidation (LTO), Middle Temperature Reactions (MTR) and High Temperature Oxidation (HTO). LTO reactions occur below 300ºC (573.15 K) as a result of injected oxygen reaction with oil. It produces water, partially oxygenated compounds and carbon oxides. MTR occurs between 300º – 400ºC (573.15– 673.15 K) and show the characteristic negative temperature region where oxygen consumption decreases as temperature increases. More coke (carboneous material) deposits on the rock matrix during this reaction period. HTO reactions occur above 400ºC (673.15 K) as a result of reaction between injected air and deposited coke. Fuel combustion occurs during this period and it produces carbon dioxide, carbon monoxide and water as its main products. In this study, kinetic experiments were conducted at 100, 150, 200 and 250 psig to study the in situ combustion kinetics of Bati Raman oil. In addition effect of pressure on the isoconversional analysis was investigated. The ramped temperature oxidation method was employed, and the produced gases were analyzed for the oxygen and carbon oxides in the effluent gas composition. A plot of gas composition versus time at all heating rates for all operating pressures give a curve that shows the three regions of the three major reactions that take place during crude oil oxidation namely; LTO, MTR and HTO. Using the gas composition plots at various heating rates, it is observed that peak oxygen consumption increases with increasing heating rate. Conventional methods of kinetic studies employ straight-line approach for kinetic data analysis. Activation energy values are estimated for high temperature oxidation region by Fassihi's method. For this method activation energy values generally decrease with increasing heating rate and increase with increasing pressure.

The isoconversional technique which is model-free and deconvolve multi-step reactions naturally is also used in the calculation of activation energy in the high temperature region and compared with those obtained with the Fassihi method. The Fassihi method activation energy values are generally higher than those estimated with the isoconversional method. Pressure effect on activation energy is studied using the isoconversional fingerprints generated at different pressures for consumed oxygen with the isoconversional method. The isoconversional fingerprint comparisons show that increase in pressure has a corresponding activation energy increase in estimated values for Bati Raman crude in HTO region. In addition, reaction models were formulated for all operating pressures. Finally, using the various fingerprints obtained at different pressures, Bati Raman crude oil is viewed as a good candidate for combustion.

**BATI RAMAN PETROLÜNÜN YERİNDE YANMA KİNETİĞİNE BASINCIN ETKİSİNİN ALIŞILAGELMİŞ VE EŞDÖNÜŞÜM YÖNTEMLERİ İLE İNCELENMESİ**

## ÖZET


Ham petroller özgül ağırlıklarına göre genellikle üç kategoriye ayrılırlar; ağır petrol ($10^o$ – $20^o$ API), orta düzey petrol ($20^o$ – $30^o$ API) veya hafif petrol (> $30^o$ API). API dereceleri 10'dan düşük petroller extra ağır petrol (bitümen) olarak adlandırılmakla birlikte bu petrollerin akmazlıkları oldukça yüksektir. Ağır petrollerin moleküler ağırlıkları yüksektir ve daha büyük bileşenleri içermekle birlikte akmazlıkları yüksektir (> 100cp). Alışılagelmiş petroller (hafif petroller) dünya petrol kaynalarının sadece %30'unu içerirler. Bu nedenle teknolojinin ve kaynakların, dünyanın çeşitli yerlerindeki, bol ağır petrol ve bitümen kaynaklarının çıkartılmasına yoğunlaşması beklenir. Ağır petrol ve bitümen kaynaklarının çıkartılmasına kullanılar mevcut yöntemler soğuk ve ısıl yöntemler olarak ikiye ayrılır.

Akmazlığı çok yüksek petroller için, akmazlığı düşürmeyi hedefleyen ısıl yöntemler tercih edilir. Isıl yöntemler buhar basma, yerinde yanma ve sıcak su basmayı kapsar. Diğer yandan, akmazlığı daha düşük ağır petroller içi madencilik, su basma gibi soğuk yöntemler uygulanır. Yüzey madenciliği rezervuar koşullarında mobilitesi olmayan bitümen çıkarımında tercih edilirken, su basma Kuzey Denizi gibi ağır petrollerin akmazlığı daha düşük olduğu yerlerde tercih edilir.

En yaygın kullanılan ısıl yöntem buhar basma, bir enjeksiyon kuyusundan buharın rezervuara iletimi ve buharın etkisi ile mobilitesi artan petrolün üretim kuyularından üretilmesini içerir. Buhar basma ile ilişkili en önemli problem ısı kayıplarıdır. Isı kayıpları esas olarak buharı kuyuya ulaştıran yüzey hatlarında, kuyu içerisinde kuyu boyunca ve rezervuarda üst ve alt formasyonlara gerçekleşir. Buna ek olarak göreli olarak kalın rezervuarlara yerçekimi ardalanması karşılaşılan diğer önemli bir problemdir. Uzun süredir bilinen yerinde yanma yöntemi buhar basma yönteminin bir çok sınırlamasını içermemektedir. Temel olarak kuru ileri basma şeklinde uygulanır. Bu uygulamada kuru buhar ile rezervuar süpürülür. Diğer bir yandan ıslak ileri yanma yönteminde hava ve su beraber veya sırayla basılırlar. Buradaki amaç geride kalan ısıyı su yardımı ile süpürüp taşımaktır. Diğer bir yöntem ise tersinir yanmadır. Bu yöntemde basılan hava ve yanma cephesi zıt yönlerde haraket ederler.

Yerinde yanmanın en önemli avantajı ısının yer altında üretilmesi ve yanma ürünlerini yer altında kalmasıdır. Yanma için gerekli hava ücretsiz olmakla birlikte heryerde ulaşılabilirdir – karada veya suda. Ancak yerinde yanma prosesi karmaşık olmakla birlikte mühendisliği zordur; kinetik modellerinin kurulması ve yanma özelliklerinin anlaşılması için birçok laboratuvar çalışması gereklidir.

Bu çalışmanın temel amaçları; Türkiyenin güneydoğusunda yer alan Batı Raman sahasının $12^o$ API'lık ağır petrolü için yanma kinetiği reaksiyon modelini

oluşturmak, basıncın eş-dönüşüm yöntemi üzerine etkisini incelemek ve kullanılan petrolün yanmaya uygun olup olmadığını eş dönüşüm yöntemi ile incelemektir.

Literatüredeki yanma kinetiği çalışmaları alışılagelmiş yöntemler ve eş dönüşüm yöntemleri olarak iki gruna ayrılabilir. Tadema (1959), Bousaid ve Ramey (1968) ve Fassihi (1981) tarafından gerçekleştirilen yerinde yanma kinetik çalışmalarının hepsi bir tür eğri-çakıştırma yöntemine dayanmaktadır. Bu çalışmalarda, reaksiyonlar gruplanır ve bir veya birden fazla reaksiyona indirgenirler. Ancak gerçekte yanma birçok karmaşık reaksiyonu içermektedir.

Eş-dönüşüm yöntemi ise modelden bağımsız bir yöntem sunarak, karmaşık reaksiyon modelini devre dışı bırakarak aktivasyon enerjisinin tahminin sağlar. Ayrıca eş dönüşüm yöntemi kullanarak bir petrolün yanmaya uygun olup olmadığı incelenebilir. Daha önce geliştirilen alışılagelmiş ve eş dönüşüm yöntemleri üç grup reaksiyona işaret ederler. Bu reaksiyonlar düşük sıcaklıkta oksidasyon (DSO), orta sıcaklıktaki reaksiyonlar (OSO) ve yüksek sıcaklıkta oksidasyondur (YSO). LTO reaksiyonları petrol ve oksijenin 300ºC altındaki reaksiyonlarıdır.Bu reaksiyonlar su ve kısmı olarak oksitlenmiş bileşenler ve carbon oksitler üretir. Orta sıcaklıktaki reaksiyonlar 300º-400ºC (573.15– 673.15 K) arasında gerçekleşirler ve sıcaklığın artarken, oksijen tüketiminin azaldığı negatif sıcaklık gradyanı bölgesi içerir. Bu reaksiyonlar sırasında kok katı kayaç matrisi üzerine çökelir. HTO reaksiyonlar çökelen kokun oksijenle reaksiyonu sonucu oluşur ve 400ºC'nin (673.15 K) üzerinde gerçekleşir. Yakıtın (kok) yanması bu dönemde gerçekleşir ve karbonmonoksit, kardondioksit ve su, bu dönemin en önemli ürünleridir. HTO reaksiyonları ısı üreten reaksiyonlardır.

Bu çalışmada 100, 150, 200 ve 250 psig basınç altında ve farklı ısıtma hızlarında deneyler gerçekleştirilmiş ve Batı Raman petrolünün yanma kinetiği irdelenmiş, buna ek olarak basıncın eş dönüşüm yöntemi üzerine etkisi incelenmiştir. Gerçekleştirilen deneylerde sıcaklık artırımlı oksidasyon yöntemi uygulanmış ve üretilen gazlardan karbon oksitler ve oksijen, sıcaklık ölçümleri ile birlikte analiz edilmiştir. Bu deneylerde örnek (petrol, kum ve su karışımı) reaktörün içerisine konulur. Ardından reaktör fırının içine yerleştrilir ve sıcaklık daha önceden belirlenen ısıtma hızına göre ısıtılır. Reaktör içerisine yerleştirilen sıcaklık sensörleri aracılığıyla sıcaklık deney boyunca kayıt edilir. Deneyler boyunda reaktöre sabit debide hava basılır. Rektör içerisinde sıcaklığın artmasıyla birlikte öncelikle su buharlaşır. Ardından petrolün ayrışması başlar ve sıcaklık yeterince yükselince kinetik reaksiyonları gerçekleşir. Sistem basıncı, geri basınç regülatörü sayesinde kontrol edilir. Reaktörden çıkan gaz bir dizi filtreden geçerek sudan, yoğuşan hidrokarbonlardan ve parçaçıklardan temizlenir ve çıkan gazın içerindeki $CO_2$, CO, $O_2$ ve $CH_4$ derişimleri kayıt edilir.

Elde edilen oksijen tüketim verileri zamana göre çizildiğinde bütün ısıtma hızlarında ve bütün basınçlarda üç ana reaksiyon bölgesi olduğu görülmüştür: DSO, OSO sıcaklıktaki reaksiyonlar ve YSO. Isıtma hızı arttıkça oksijen tüketiminin ulaştığı maksimum değer artmaktadır.

Alışılagelmiş yöntemler, doğrusal eğri-çakıştırma yöntemlerini kullanmaktadır. Aktivasyon enerjisi YSO bölgesi için Fassihi modeli kullanılarak hesaplanmıştır. Fassihi yöntemi ile elde edilen aktivasyon değerleri irdelendiğinde, artan ısıtma

hızıyla hesaplanan aktivasyon enerjisi değerlerinin azaldığı, artan basınçla birlikte arttığı gözlemlenmiştir. Buna ilaveten modeleden bağımsız ve reaksiyon gruplarını ayrıştırabilen eş-dönüşüm yöntemi kullanılarak aktivasyon enerjisi hesaplanmış ve Fassihi yönteminden elde edilen değerlerle kıyaslanmıştır. Fassihi yöntemi ile elde edilen aktivasyon enerjisi değerlerinin daha yüksek olduğu görülmüştür.

Basıncın etkisi eş-dönüşüm yöntemi ile hem oksijen ölçümleri hem de karbonoksit ölçümleri kullanılarak incelenmiştir. Eş-dönüşüm eğrileri farklı basınçlarda karşılaştırıldığında, Batı Raman petrolünün YSO bölgesinde basıncın artmasıyla daha yüksek aktivasyon enerjilerinin hesaplandığı görülmüştür. Bunlara ek olarak, bütün basınçlar için reaksiyon modelleri oluşturulmuştur. Son olarak eş dönüşüm eğrileri değerlendirilerek Batı Raman petrolünün yanma için iyi bir aday olduğu sonucuna varılmıştır.

## 1. INTRODUCTION

Crude oils are often grouped into three main categories based on specific gravity range as: heavy oil (10º-20º API), intermediate oil (20º-30º API) and light oil (>30º API). One of the greatest hydrocarbon resources in the world is heavy oil and bitumen (oil sands). Heavy oils are highly viscous (>100 cP) and consist of high-density napthenes, aromatics, and heteroatoms that are poor in conventional oils. Bitumen (oil sands) are extremely dense hydrocarbons (<10º API) having viscosities around 10000 cP. A fourth classification of crude oils is the so-called extra heavy oil (Schlumberger, 2006). The API gravity is less than 10 and share many attributes of bitumen (oil sands) although bitumen are denser. Figure 1.1 shows the United States Geological Survey (USGS) percentage allocations for total oil reserves (conventional and unconventional oils). From Figure 1.1 we notice that heavy oil resources are very abundant and therefore technology and research must be focused on how to extract these resources for human consumption. Figures 1.2 and 1.3 gives the various regional distribution of heavy oil and natural bitumen resources in the world. It is apparent that most of the heavy oil and bitumen resources are concentrated in the Americas and interestingly the total combined heavy oil reserves of Canada and Venezuela is much more than the conventional oil resource of Saudi Arabia.

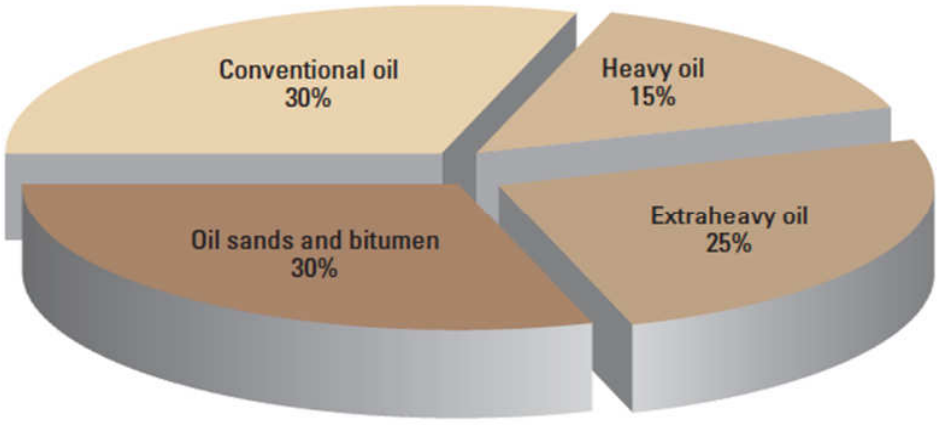


**Figure 1.1:** World oil reserves distribution (Schlumberger, 2006).

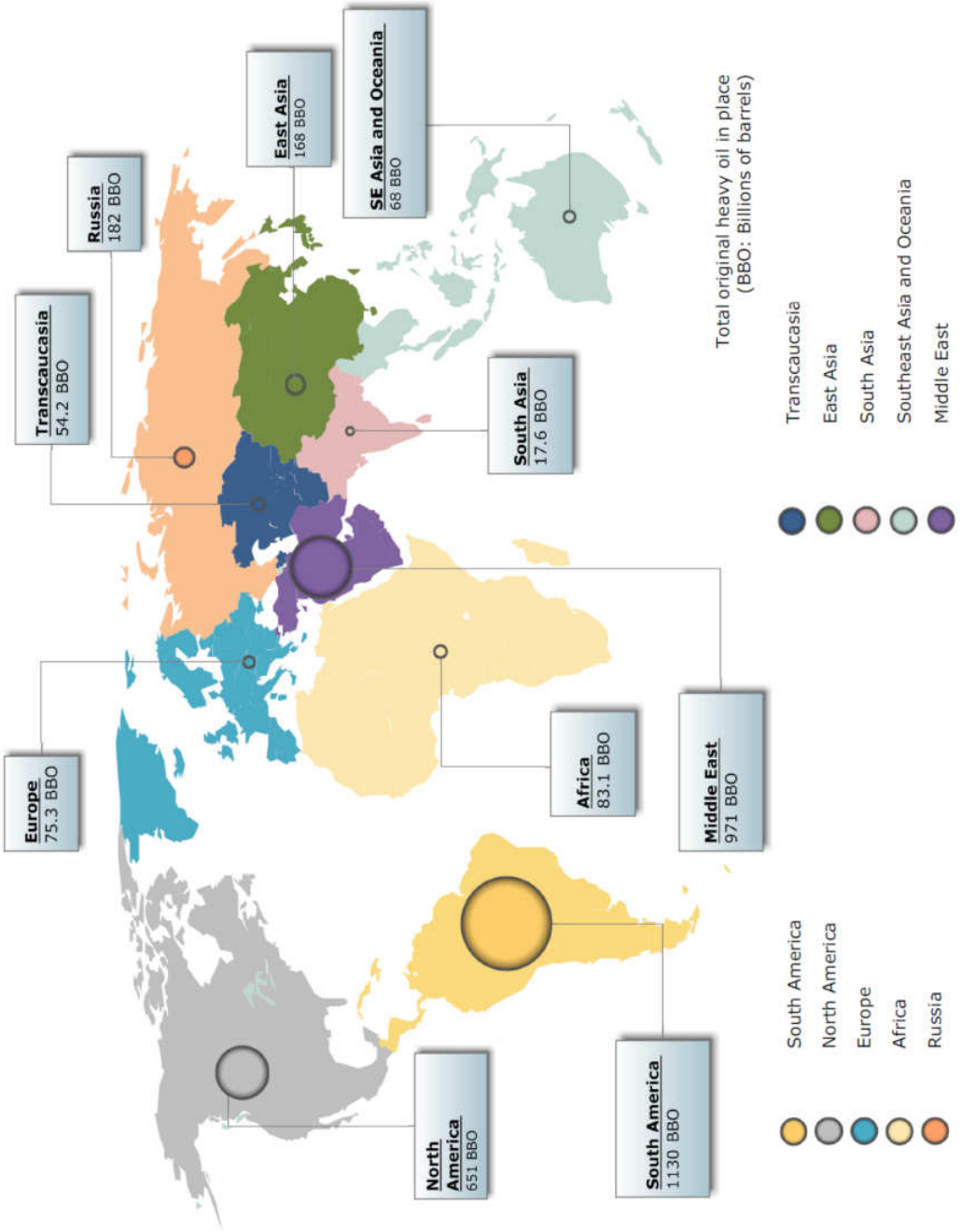


**Figure 1.2:** Heavy oil resources in the world (Çınar, 2011).

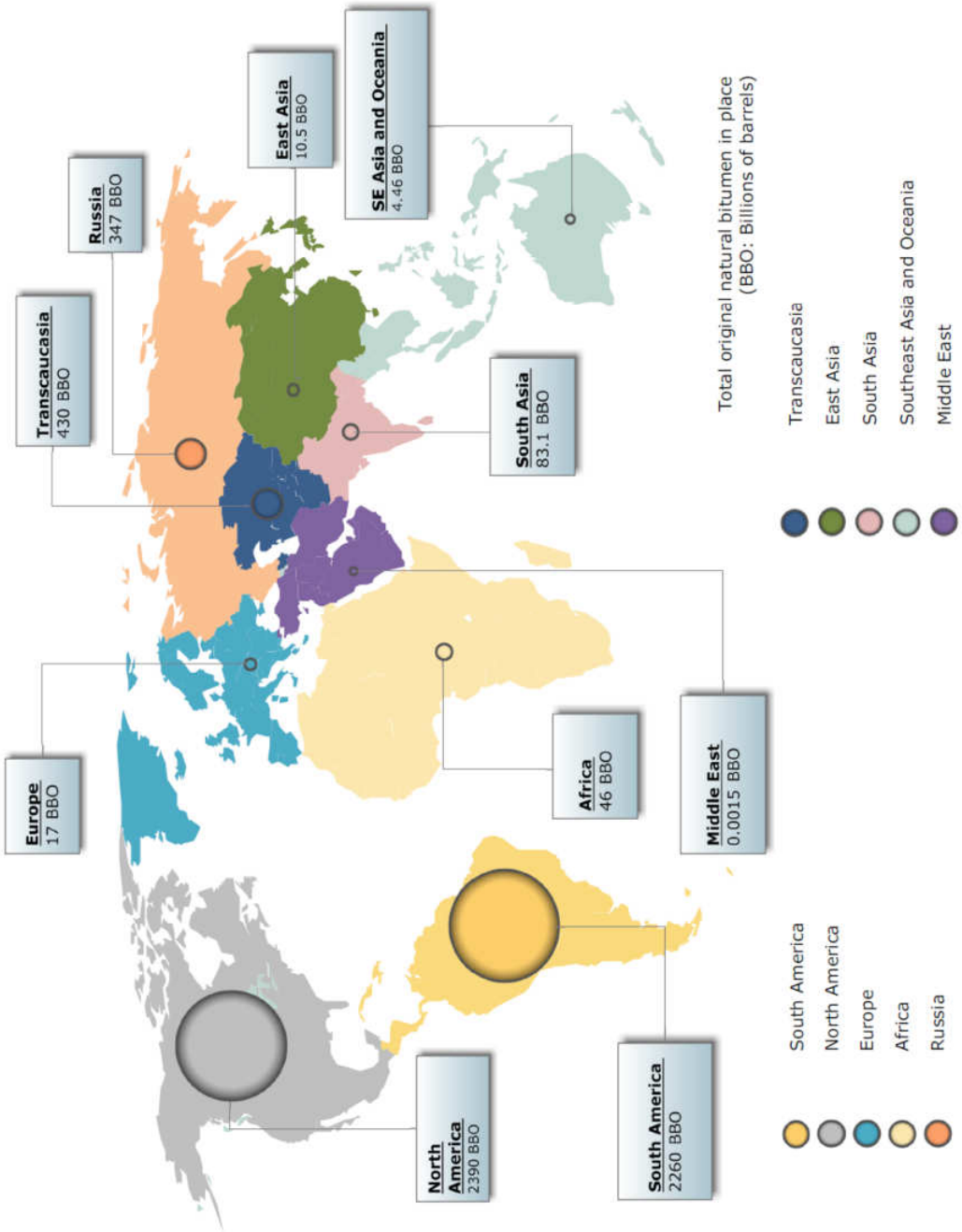


**Figure 1.3:** Bitumen resources in the world (Çınar, 2011).

## 1.1 Recovery Methods for Heavy Oil and Natural Bitumen

Most heavy oil and natural bitumen are recovered via enhanced oil recovery methods (EOR). Heavy oil resources are naturally recovered by thermal and non-thermal methods depending on the viscosity of the oil within the reservoir. For very highly viscous crude oils, thermal methods i.e. steam injection, hot water flooding, in situ combustion are employed. Heat is either generated on the surface and transferred into the reservoir as in the cases of steam injection, hot water flooding or the heat is generated within the reservoir through the process of in situ combustion.

### 1.1.1 Mining

Mining process is applied extensively in Canada where most mining of heavy oil resources occurs in open pit mines. However, in Russia subsurface mining has been reported (Meyerhoff and Meyer, 1987). The open pit method is used exclusively in Canada due to the vast amount of heavy oil and bitumen resources and the economic considerations. Most of the bitumen is mined by tracks and transported to processing sites by trucks due to the viscous nature of the bitumen. Bitumen can also be transported by pipeline if it is diluted with a condensate. In the processing plants, warm water is used to separate bitumen from the sand and diluted with lighter hydrocarbons to form a synthetic crude.

### 1.1.2 Waterflooding

Waterflooding has been employed in some heavy oil reservoirs around the world with some amount of success. In the United Kingdom continental shelf where viscosity of heavy oils range from 10-100 cP, waterflooding has been extremely successful (Etebar, 1995). Viscous fingering, however, is a major issue in heavy oil reservoirs and appropriate precautions must be taken. As the viscosity increases, the recovery factor of waterflooding decreases.

### 1.1.3 Steam stimulation (Huff n Puff)

This method was discovered accidentally by Shell in Venezuela during heavy oil production in Lake Maracaibo area. It is a single well method that involves three main stages as shown in Figure 1.4. The first stage involves the injection of steam into the reservoir. In the second stage, time is allowed for the steam to diffuse into

the reservoir and heat the heavy oil in place. Finally, the heated oil is produced along with water to the surface from the same well and then separated.

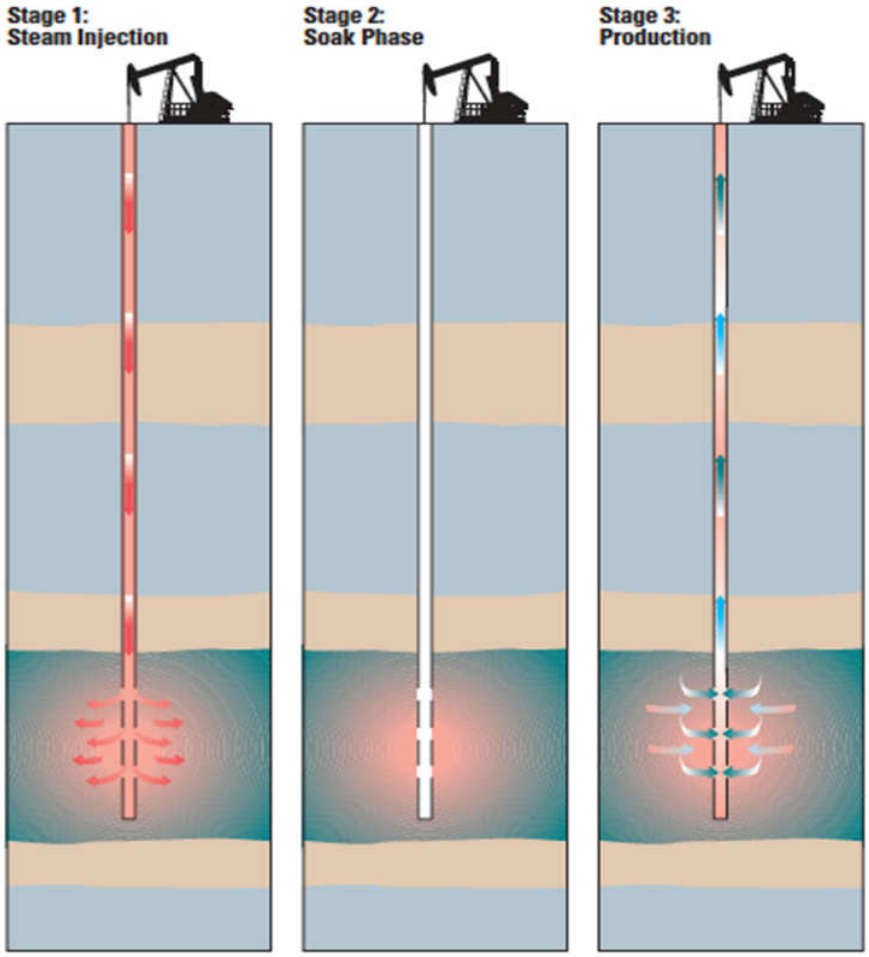


**Figure 1.4:** Schematic representation of Huff n Puff Method (Schlumberger, 2006).

### 1.1.4 Steam flooding

Among the thermal methods, steam flooding is the most successful and popular method used in the recovery of heavy oil. It is a multiwell process which involves the injection of surface generated steam from several injectors at various locations into the reservoir. The energy from the steam helps to heat the oil within the reservoir, reducing the oil's viscosity and hence helps the oil to move towards the producer

wells. Recovery factor is estimated at about 50% OOIP. The main challenge with steamflooding stems from gravity override. Owing to the density difference between steam and oil, steam has a tendency of rising above oil within the reservoir. The oil below the steam does not get affected much with the heat from the steam and therefore gets left behind or recovers slowly from the condensed hot water from the steam. Early breakthrough of steam front into producer wells is also a major challenge in steam flooding process. Another limiting factor is the depth; as the depth increases heat losses from the injection well to the surrounding formation increases.

### 1.1.5 In situ combustion

In situ combustion (ISC), which is also known in the literature, as fire flooding or air injection is the oldest EOR thermal method. The idea of in situ combustion was granted a patent in 1923 (Howard, 1923). Based on the respective directions of front propagation and airflow, in situ combustion is characterized as either a forward process, when the combustion front advances in the same direction as airflow or reverse, when the front moves against the airflow (Brigham and Castanier, 2003). Forward is applied in two forms namely:

- Forward dry combustion
- Forward wet combustion

In dry forward combustion which is the most common, air is injected into a heavy oil reservoir through selected injection wells to create a combustion front within the reservoir, then ignition is initiated and a combustion front is propagated through the reservoir with the continuous injection of air. The heat generated within the reservoir reduces the viscosity of the oil and thereby increases the oil production rate and recovery.

Wet combustion is the second form of forward in situ combustion. Regarding this method, water is injected concurrently or alternatively with air to get more efficient heat utilization. The purpose of injecting water is to transport heat from the burned zone to the colder regions downstream of the combustion front from rising steam generated from the heated water. This variation of in situ combustion is most suitable for thin reservoirs, where heat loss to adjacent formations is significant (Dietz and Weijdema, 1963).

The second type of in situ combustion is the reverse combustion process. In this process, the injected air and the burning zone move counter currently. This method is suitable for highly viscous crudes such as tars (Dietz and Weijdema, 1963).

Figure 1.5 shows a schematic representation of the various zones formed after air injection in a dry-forward in situ combustion process. Figure 1.5 shows that as the combustion front propagates through the reservoir, different zones with varying temperatures and saturations are formed within the reservoir.

The first zone is termed as the burned zone. This is the zone swept by the combustion and is saturated with air. The temperature in this zone is usually very high. The second zone is the combustion zone. This is where most reactions take place. As the temperature within the reservoir exceeds about 300$^{o}$C (573.15K), the oil may undergo a process called pyrolysis to form a volatile fraction and a low-volatility heavy residue (coke). The volatile fraction is carried in the gas stream to upgrade the original crude oil while the non-volatile heavy residue is burned as fuel to sustain the combustion process (Castanier and Brigham, 2003). The third zone is the coking zone. Coke is a carboneous substance laid down ahead of the combustion zone to be burned to sustain the combustion process.

It forms as a result of some injected oxygen breaking through the combustion front and reacting with crude oil (Burger and Suhuquet, 1976). The fourth zone is the steam zone. This zone results from the vaporization of water in the reservoir as well as produced water from the combustion zone.

A fifth zone, the water bank forms ahead of the steam zone from the condensing steam from the fourth zone. The last zone is the oil bank where the mobilized oil accumulates. A comprehensive review of in situ combustion projects have been compiled and compared in the literature (Farouq Ali, 1972; Sarathi, 1999).

In situ combustion is difficult to engineer due to the complexity of the process, and it also requires extensive laboratory studies prior to field pilot tests.

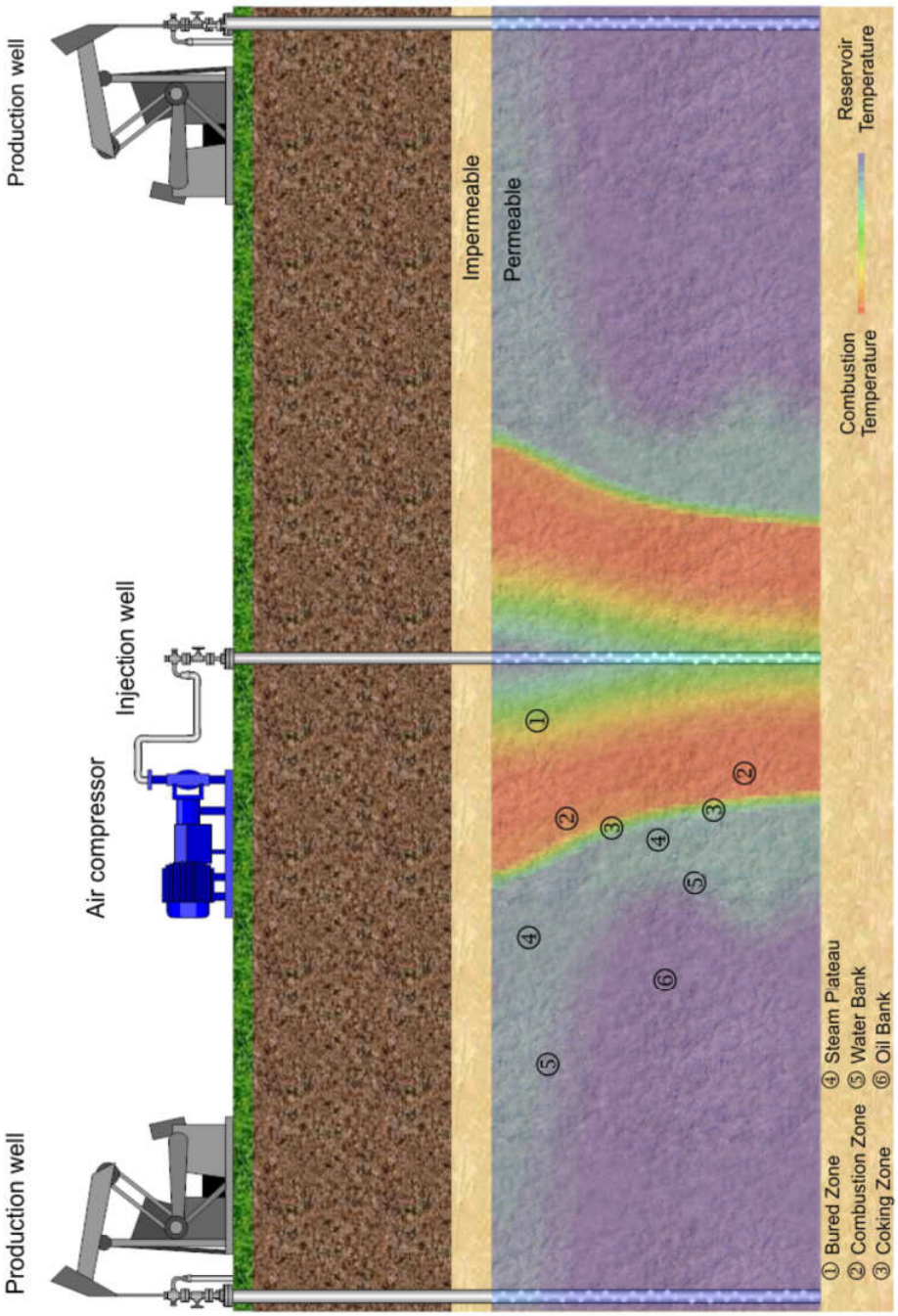


**Figure 1.5:** In situ combustion schematic - showing various zones (Çınar, 2011).

### 1.1.6 Carbon dioxide flooding

Carbon dioxide flooding is a popular gas injection method in EOR. Depending on the reservoir pressure, $CO_2$ flooding is applied as a miscible or immiscible process. Miscible fluids form a single homogenous phase when mixed together (eg. $CO_2$ and

oil). Immiscible fluids separate into two distinct phases when mixed together (eg. Oil and water). The success of $CO_2$ projects, however, lies in finding a cheap source of carbon dioxide. The Bati Raman oil field in the South-Eastern part of Turkey which was discovered in 1961 and its the largest oil field in Turkey is currently undergoing an immiscible $CO_2$ flooding process. Owing to the viscous nature of the oil with API of 12º and less reservoir pressures, the Turkish Petroleum Corporation chose the immiscible $CO_2$ flooding project in 1986 as a tertiary recovery method. The main source of carbon dioxide to the Bati Raman field is from the vast Dodan field which lies 90 km from Bati Raman. Recovery factor by $CO_2$ flooding from Bati Raman is estimated at around 7% of 1.85 MMMbbl OOIP to date which is a limited success considering the vast resources of Bati Raman oil field.

### 1.2 Statement of the Problem

Depending on the viscosity and temperature conditions within a heavy oil reservoir various types of recovery methods are available for its extraction. However, economic costs as well as technology and reservoir characteristics become critical in choosing which method to use for heavy oil production. In situ combustion process involves the generation of heat in situ and containment of combustion products within the reservoir (Moore et al., 1997). Upgrading of heavy oils through the burning of the heaviest parts and air utilization, which is cheap and available everywhere gives in situ combustion an added advantage. Although in situ combustion has been characterized as a high mobility ratio process, it appears to have areal stability with less fingering tendency. The reported areal sweep efficiencies have been around 50% (Farouq Ali, 1972).

Modeling of complex in situ combustion process requires an understanding of the behavior of different physical phenomena such as phase change, chemical reactivity as well as heat and mass transfer (Çınar, 2011). Knowledge of the kinetics involved in the various reactions of an in situ combustion process is essential for making meaningful predictions of the effectiveness of any combustion project. Chemical kinetics studies of crude oils help to obtain accurate data to form a reaction scheme of various reactions that occur during crude oil oxidation (Freitag and Verkoczy, 2005; Mamora, 1993). The main objective of this project is to study the effect of pressure on combustion kinetics of Bati Raman crude oil (12ºAPI) and to compare its

kinetic parameters such as activation energy, using both conventional method given by Fassihi (1981) and an isoconversional analysis method described by Friedman (1964). Reaction scheme models for the Bati Raman crude oil are also proposed at all operating pressures used.

## 2. LITERATURE REVIEW

Various studies have been conducted in the literature on the oxidation of crude oils in porous media. The different methods used for crude oil oxidation analysis can be classified under three groups namely as; qualitative, quantitative and compositional methods.

### 2.1 Qualitative Analysis of Crude Oil Oxidation

The two main methods employed in the literature are differential thermal analysis (DTA) and thermogravimetric analysis (TGA). Tadema (1959) and Berry (1968) both employed DTA in their crude oil oxidation experiments using an oil sand. In DTA experiments, a crude oil and sand mixture is heated at a uniform heat rate while air is passed through the mixture. The amount of heat released affects temperature, which is recorded on a thermogram.

Another method of qualitative analysis is thermogravimetric analysis (TGA), which involves heating a crude oil and sand sample at a constant heat rate in the presence of flowing air. Here, the resulting curve of weight change versus time or temperature gives the TGA thermogram. A coupling of TGA and DTA thermograms also indicates the occurrence of at least two reactions at different temperatures (Bae, 1977). The TGA and DTA data can be used for determining kinetic parameters such as activation energy, heat of reaction as indicated extensively by Sarathi (1998).

### 2.2 Quantitative Analysis of Oxidation of Crude Oil

This method of analysis is based on produced gas during crude oil oxidation. This is usually referred to as effluent gas analysis (EGA). EGA studies involve crude oil oxidation at a constant temperature or rising temperature. Isothermal oxidation experiments were conducted by Bousaid and Ramey (1968), Weijdema (1968), and other researchers. Results from these experiments showed that the rate of carbon

combustion depends on carbon concentration, oxygen partial pressure, and combustion temperature.

Non-isothermal EGA studies of crude oil oxidation on the other hand uses programmed linear temperature rise – ramped temperature oxidation (RTO). Studies done using RTO techniques by Burger and Suhuquet (1972), Fassihi (1981), Cinar (2011) and other researchers also confirm existence of two peaks in crude oil oxidation. The first reaction termed low temperature oxidation (LTO) usually occurs at about 300ºC (573.15K). The second reaction termed as high temperature oxidation (HTO) also has a peak at about 400ºC (673.15). Later Fassihi (1984a; 1984b) proposed an oxidation reaction model which emphasized the existence of a third reaction known as medium temperature reaction (MTR).

### 2.3 Compositional Analysis

This method of crude oil analysis is used to determine the various components of a crude oil sample by either oxidation or thermal cracking methods. Studies done by various investigators revealed several reaction schemes in crude oil breakdown.

Hayashitani (1978) deduced from his experiments in thermal cracking of Athabasca bitumen consisted of the following first order reactions in reaction scheme 2.1;

$$Maltenes \rightarrow Asphalthenes$$
$$Asphalthenes \rightarrow Coke$$
$$Asphalthenes \rightarrow Gas$$

**Reaction Scheme 2.1**: Cracking scheme proposed by Hayashitani (1978).

Adegbesan (1982) using the SARA analysis method conducted LTO experiments on Athabasca Bitumen and proposed the following reaction scheme 2.2 for crude oil oxidation;

$$Maltenes + Oxygen \rightarrow Asphalthenes$$
$$Asphalthenes + Oxygen \rightarrow Coke$$

**Reaction Scheme 2.2**: Scheme proposed by Adegbesan (1982).

SARA analysis separate crude oil components based on solubility of the different components by various solvents. The crude oil components are saturates, aromatics, resins, and asphalthenes (SARA).

Belgrave et al. (1993) also proposed reaction scheme 2.3 for Athabasca bitumen by mainly combining the previous reaction schemes of Hayashitani and Adegbesan in his oxidation and thermal cracking studies.

$$Maltenes \rightarrow Asphalthenes$$
$$Asphalthenes \rightarrow Coke$$
$$Ashalthenes \rightarrow Gas$$
$$Maltenes + Oxygen \rightarrow Asphalthenes$$
$$Asphalthenes + Oxygen \rightarrow Coke$$
$$Asphalthenes + Oxygen \rightarrow Gas$$
$$Coke + O_2 \rightarrow CO_2 + CO + H_2O$$

**Reaction Scheme 2.3**: Scheme proposed by Belgrave et al., (1993).

In this reaction scheme, oil is separated into fractions and each reaction is analyzed individually.

### 2.4 Isoconversional Method

Most conventional studies in the literature assume a sort of kinetic model in the calculation of kinetic parameters. However straight line-fitting models can introduce errors in the analysis procedure since hydrocarbon combustion involves lots of other complex reactions (Semenov, 1935).

Isoconversional methods however, provides model free methods for the calculation of activation energies (Vyazovkin, 1997). Isoconversional methods leads to isoconversional fingerprint which is a plot of activation energy versus conversion. Conversion values are estimated based on oxygen consumption as measured at the outlet of the kinetic cell. Isoconversional fingerprint indicates the change in reaction mechanism in the extent of conversion or average temperature.

In addition the isoconversional methods provides a screening criteria for the determination of good and bad candidates for combustion (Çınar et al., 2011) based on combustion kinetics. To apply the isoconversional approach in crude oil kinetics studies, a general workflow plan by Kovscek et al., (2013) shown in Figure 2.1 was proposed.

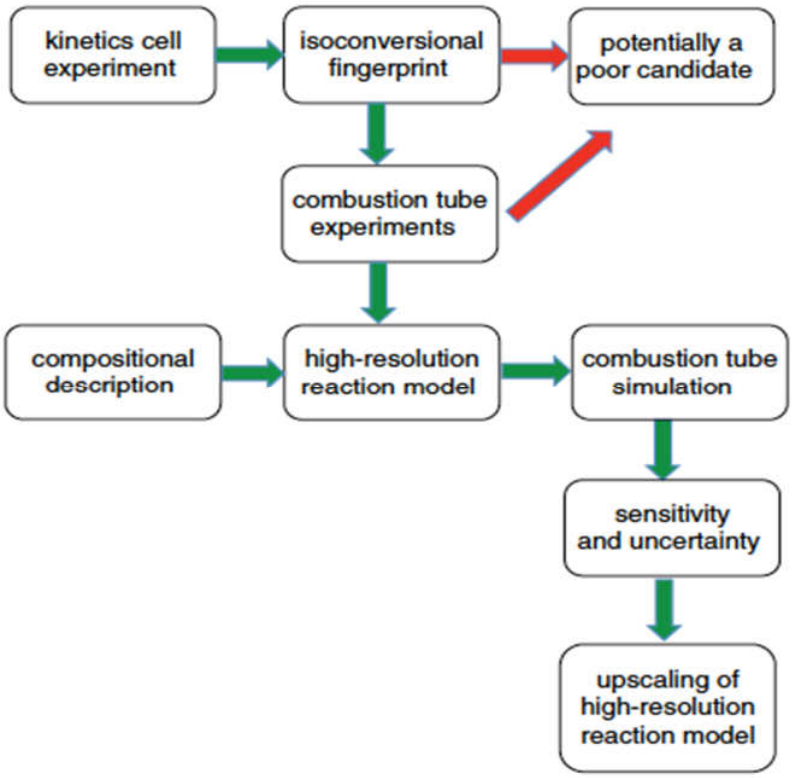


**Figure 2.1:** Proposed workflow for isoconversional analysis (Kovscek et al., 2013).

The workflow entails that we begin with crude oil oxidation in a kinetic cell with a series of experiments. Then we can generate an isoconversional fingerprint as Figures 2.2 and 2.3. Based on the fingerprints screens, we can determine if the oil is a good candidate or poor candidate for combustion front propagation. If the crude oil turns out as poor candidate (red arrows) for combustion front propagation, we can use combustion tube experiments, which are on a much larger scale to confirm the kinetic experiment results. A crude oil that turns out to be a good candidate (green arrows) for combustion front propagation based on kinetic cell and combustion tube experiments can then be processed further along the workflow plan. A detailed compositional and PVT properties of the oil are obtained. An experimental reaction model is proposed from the kinetic cell and combustion tube results, which will be compared with a simulated reaction model. Finally, up scaling of the reaction model is done to project it from laboratory to field scale. An isoconversional fingerprint shows changing dominant reactions on a plot of effective activation energy with conversion or average temperature. The smooth transition from the negative temperature region (NTGR) in Figure 2.2 (conversion of 0.2-0.5) to HTO

(conversion of 0.6-0.9) is a typical indication of a good candidate for combustion (Çınar, 2011). Also for good candidates for combustion, the effective activation energy value obtained in the LTO region is generally lower than the HTO region.

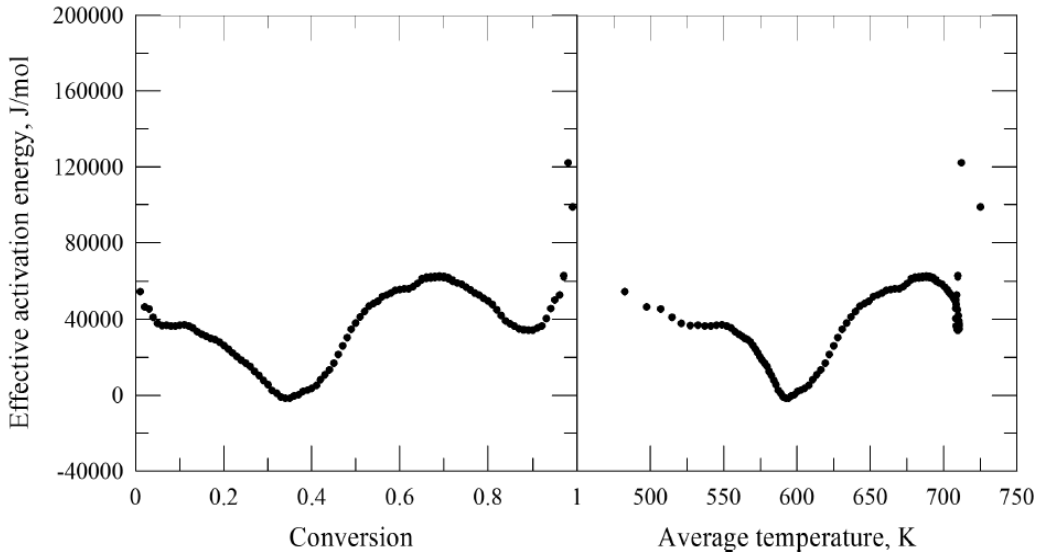


**Figure 2.2:** Isoconversional fingerprint of a well burning crude oil (Çınar et al., 2011).

Poor candidates for combustion however, exhibit significant barriers in the LTO region. Figure 2.3 also shows the isoconversional fingerprint for a poor or bad crude oil for combustion.

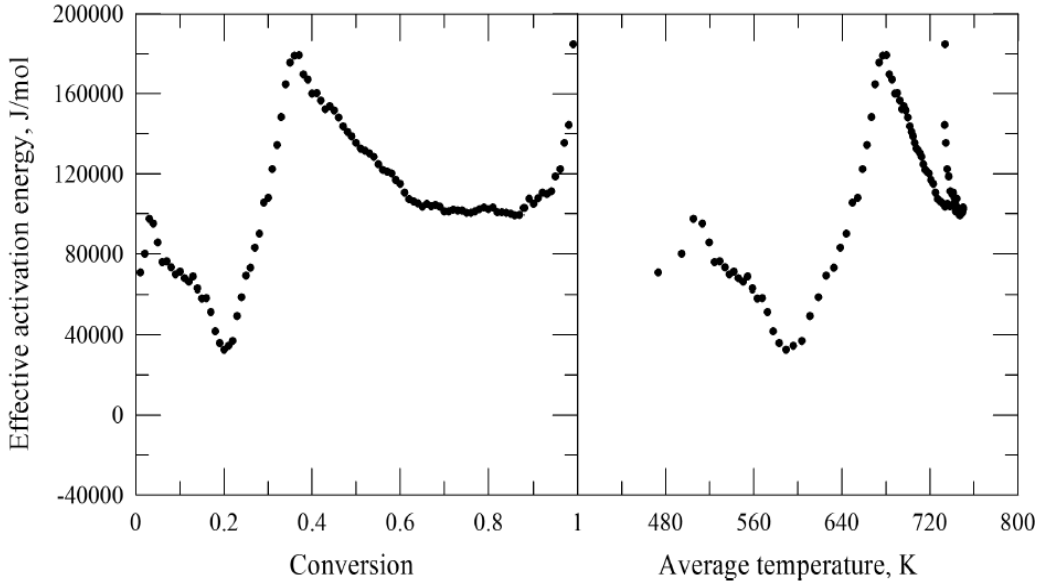


**Figure 2.3:** Isoconversional fingerprint of a poor candidate for combustion (Çınar et al., 2011).

It is observed from Figure 2.3 that the NTGR (conversion of 0.2 to 0.4) develops a high activation energy barrier and does not transition smoothly into the HTO region, as was the case in Figure 2.2. A crude oil that exhibits a high-energy barrier in NTGR in its fingerprint is regarded as a poor candidate for combustion per the isoconversional analysis method.

### 2.5 In Situ Combustion Reactions

Kinetic studies conducted on crude oil oxidation in porous media by various investigators: Bousaid and Ramey (1968), Weijdema (1968), Fassihi (1981), and several other investigators in the literature point to the fact that three major reactions occur during in situ combustion reaction mechanism namely (see Figure 2.4):

- Low Temperature Oxidation (LTO)
- Middle Temperature Reaction (MTR)
- High Temperature Oxidation (HTO)

#### 2.5.1 Low temperature oxidation

Low temperature oxidation reactions occur at temperatures below 300$^{o}$C (573.15 K) as a result of oxygen (injected air) during in situ combustion process. Oxygen may be available downstream after air injection or ignition (Moss et al, 1959; Ramey, 1959; Tadema and Weijdema, 1970). An LTO reaction yields water and partially oxygenated hydrocarbons such as carboxylic acids, aldehydes, ketones (Burger and Suhuquet, 1972). LTO reactions are regarded as oxygen addition reactions. Dabbous and Fulton (1974) showed that during LTO reactions, diffusion of oxygen into the oil phase is faster than the oxidation process. LTO reactions are highly complex and not very well understood. Studies point to the fact that during LTO, asphalthene content of the oil is increased whilst aromatic and resin contents decrease (Babu and Cormack, 1984). Alexander et al. (1972) also found that LTO reactions increase the viscosity and boiling range of the oil. Light oils are generally more susceptible to LTO than are heavy oils. In heavy oil reservoirs, LTO tends to be more pronounced when oxygen, rather than air is injected into such reservoirs. LTO reactions are generally evidenced by a rapid increase in the oxygen uptake rate as well as the

production of carbon oxides. Their main characteristic feature is the decline of oxygen reaction rate even as temperature increases within the range of 300ºC-400ºC (573.15 – 673.15) Moore et al. (1997). This gives rise to the negative temperature gradient region seen on Figure 2.4.

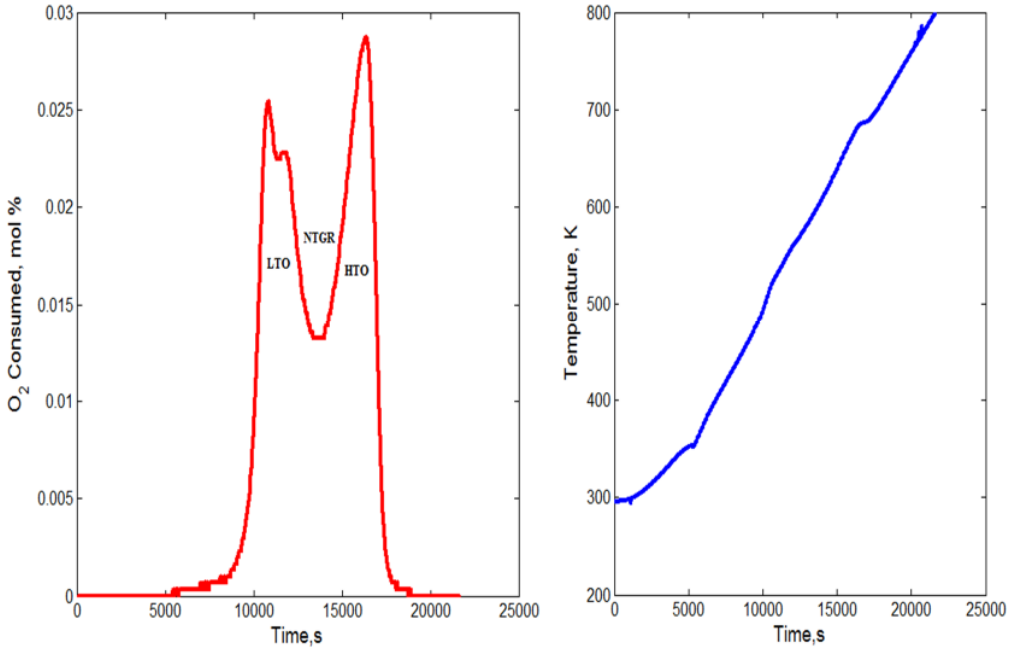


**Figure 2.4:** LTO, NTGR and HTO regions observed for 1.62 K/min (150 psig).

Fassihi et al. (1984b) observed that failure of reaction temperatures to transcend the negative temperature gradient region would lead to very low displacement efficiency. LTO of light oils does not significantly affect their mobility. However, in heavy oil reservoirs, LTO has a significant effect on mobility as both viscosity and density increase, which in turn affect heavy oil recovery. Fuel availability (coke) and air requirements for combustion increase for pre-oxidized heavy crudes at lower temperatures (< 573.15 K). During LTO reactions, certain reactive species in the oil often produce hydroperoxides intermediates, which decompose to release much heat, and can cause oil to auto ignite (Burger, 1976).

Several investigators to estimate the spontaneous ignition time for an in situ combustion project have used the heat released during LTO (Gates and Ramey, 1958; Tadema and Weijdema, 1970). LTO reactions tend to have a dominant effect on fuel deposition and composition.

### 2.5.2 Middle temperature reactions

It is generally accepted in the literature that during middle temperature reactions 300ºC – 500ºC (573.15 - 773.15 K), most oils undergo a chemical change called pyrolysis. Pyrolysis reactions lead to the deposition of a carboneous residue also referred to as coke, which serves as the main fuel for the combustion front reactions. Pyrolysis reactions are of three main kinds:

i) Dehydrogenation reactions: This leads to stripping of hydrogen atoms from the hydrocarbon molecules.

ii) Cracking: During this process the carbon-carbon bond of the heavier hydrocarbon molecules are broken which results in the formation of lower carbon number hydrocarbons

iii) Condensation reactions: This leads to an increase in the number of carbon atoms in the hydrocarbon molecule.

The type of oil determines the rate and extent of these reactions as either a straight chained or aromatic hydrocarbons. Besides, an investigation by Gates and Ramey (1958) of core samples taken from South Belridge indicates that reservoir lithology plays an important role in fuel deposition. Kinetic studies done by Bousaid and Ramey (1968) showed that the amount of fuel deposited increases with the addition of clay to the sample of oil and sand.

### 2.5.3 High temperature oxidation

HTO (combustion) reactions occur at temperatures above 400ºC (673.15 K) as a result of reactions between oxygen in the injected air and deposited coke. HTO reactions yield carbon dioxide ($CO_2$), carbon monoxide (CO) and water ($H_2O$) as by-products. Fuel combustion mostly occurs at the combustion front and therefore data from combustion tube experiments have been used to define combustion front and it's characteristics. Benham and Poettmann (1958) deduced that HTO reactions are heterogeneous and characterized by consumption of all oxygen in the gas phase. They proposed a global reaction for HTO as follows;

$$CH_n + \left[\frac{2m+1}{2(1+m)} + \frac{n}{4}\right]O_2 \rightarrow \left[\frac{1}{1+m}\right]CO + \left[\frac{m}{m+1}\right]CO_2 + \frac{n}{2}H_2O \qquad \textbf{(2.1)}$$

$m$ = mole percent ratio of produced $CO_2$ to CO

$n$ = atomic ratio of hydrogen to carbon

Cady and Satchell (1985) also assert that HTO is a surface controlled reaction and highly exothermic. The energy generated by these reactions provides the heat to sustain the combustion front.

### 2.6 Previous Kinetic Studies on Bati Raman Crude Oil

Previously, various investigators such as Bağci et al. (1987), Bağci (2005) and other investigators have studied pressure effect on Bati Raman crude oil with limestone matrix using the effluent gas with programmed temperature method (non-isothermal) HTO activation were estimated using the conventional method proposed by Fassihi (1981). Bağci et al. (1987) particularly went further in their studies by comparing the effect of matrix composition on reaction kinetics at a pressure of 25 psig for a 17.8$^o$ API oil in their study.

Bağci et al. (1987) asserts that, reaction species ratios such as $CO_2$/CO and H/C ratios were more in limestone matrix than in sandstone matrix. Infact, they conclude that, in sandstone matrix the ratios are halved that of limestone matrix. Bağci et al. (1987) and Bağci (2005) both conclude from their kinetic studies that, pressure increases with activation energy in the HTO region for Bati Raman crude oil. The various operating pressures used in both studies ranged from 5-50 psig. Injection rate of air used in both studies was reported as 1.5 liters per minute.

There are no cited works on the study of kinetics of Bati Raman crude using isoconversional analysis method as at the time of this study. In this study, pressures of 100 – 250 psig are used and air injection rate of 2 liters per minute is employed.

## 3. EXPERIMENTAL METHODS

The experimental study is based mainly on Ramped Temperature Oxidation (RTO) with effluent gas analysis approach using kinetic cell experiments. The main crude under investigation is from the Bati Raman Field in the Southeastern part of Turkey and the investigation seeks to find the effect of pressure on combustion kinetics for this crude oil along with the kinetic properties of the Bati Raman Oil. In RTO experiments, a linear heating rate is imposed under a constant pressure whilst the crude is burned with pre-programmed heating rate.

The schematic of the experimental apparatus is shown in Figure 3.1. The most important components of the system are shown in Table 3.1. The system is designed to operate and acquire data automatically without any user action during the experiment. There is a temperature limit controller and pressure relief valves to shut the system down in case of any failures. A Servomex 4200C gas analyzer is also installed to measure effluent gas from the burned crude. Due to the sensitivity of the gas analyzer and risk of damage, filters and liquid traps are installed to prevent contamination from large particles and water molecules.

The water that remains in the system from condensing gas is especially trapped with Drierite ®. The filter system does not allow particles bigger than 2 microns to pass through the mass flow rate meters. The gas analyzer measures the effluent gases through four main modules designed for $CO_2$, CO, $CH_4$ and $O_2$. Each gas is monitored individually continuously throughout the experiment. The $CO_2$, CO, $CH_4$ modules are infrared whereas that for $O_2$ is paramagnetic. Further details of the modules are described by (Çınar, 2011). There is water bath where leak testing of the kinetic cell is conducted. Relief valves are installed to depressurize the system if set pressure limits within the lines are exceeded. The various gases are removed from the system through the vents. Backpressure regulators are used in setting desired air injection pressures for the various experiments. The mass flow meters are used to set our gas injection flow in and flow out rates.

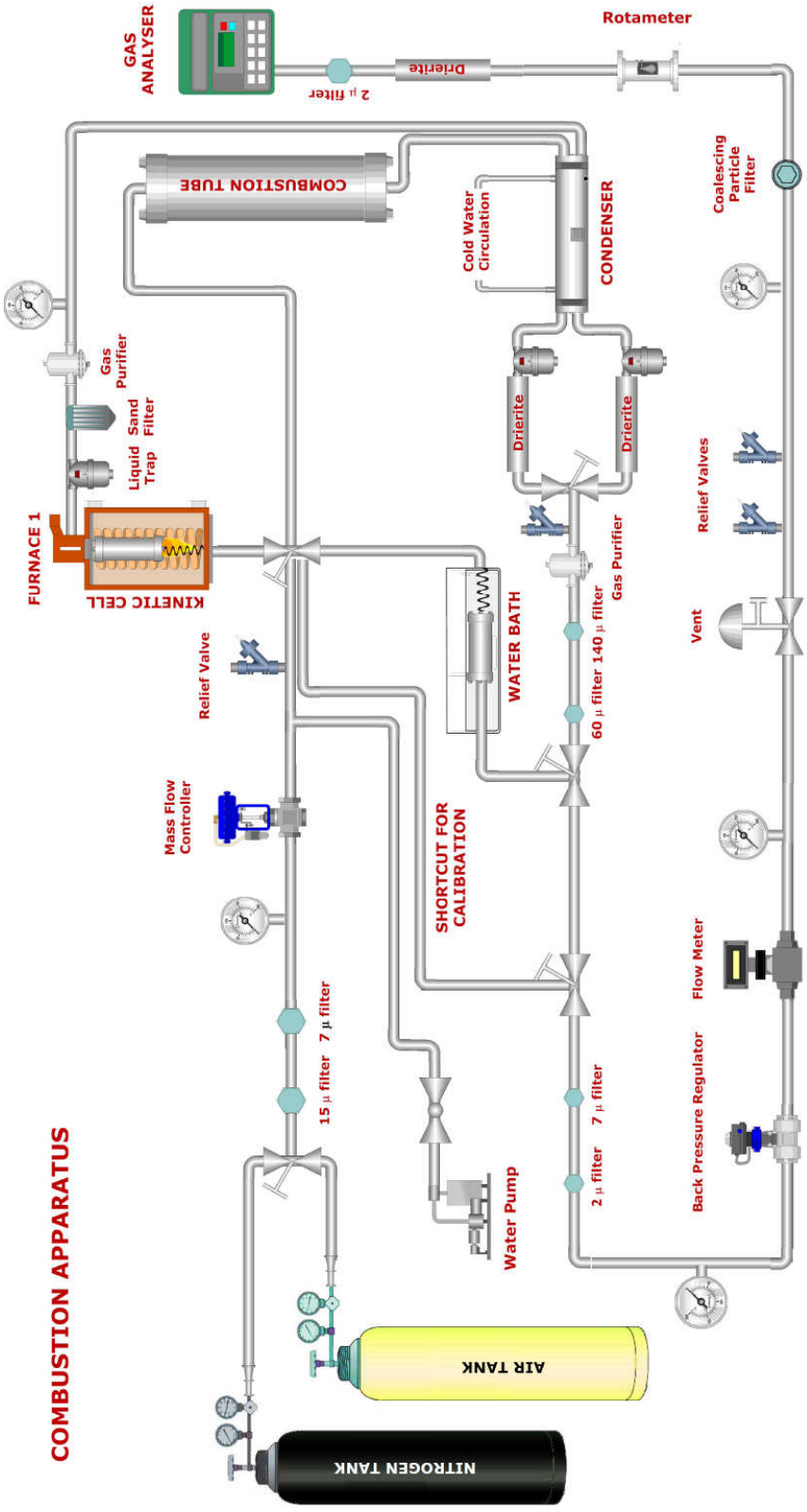


**Figure 3.1:** Schematic of kinetic experimental system (Çınar, 2011).

**Table 3.1:** Major Components of Experimental System

| Component | Manufacturer |
|---|---|
| Mass flow controller | Brooks Instrument, model 5850E |
| Gas flow meter | Brooks, F2475-002 |
| Gas analyzer | Servomex analyzer, model 4000 series |
| Temperature Controller | Omega, model CN 3261 |
| Data logger | Measurement Computing, USB-TC |
| Back pressure regulator | Hamlet H900 series |
| Relief valves | Hamlet H900 series |

### 3.1 Kinetic Cell Apparatus

The kinetic cell is a thick walled stainless steel reactor measuring 12.4 cm long and 1.8 cm in wall thickness. It has copper gaskets and stainless steel plugs to seal the top and bottom parts. Copper gaskets sit on knife-edges sealing the cell at high temperature and pressure conditions. The six screws are tightened over the upper and lower end caps to obtain the high-pressure environment desired within the cell. The thickness of the cell ensures equal distribution of heat around the packed sample during the experiments. A schematic of the kinetic cell is shown in Figure 3.2. There is a thermal well at the top of the cell to insert a thermocouple directly into the prepared sample to record the temperature within the cell during the experiment at high pressure conditions. Temperature is measured at three different points of the cell (top, bottom, middle) to check whether the temperature is uniform or not. Normally the temperature is uniform within the sample. Middle measurements are used for the analysis though all the temperature measurements are the same within the measurements errors. Temperature error of 1.1$^{o}$C (0.4%) is reported in the manual catalogue of the manufacturer (Omega industries). Gas for the experiment is usually injected from the bottom of the cell. The gas is injected through a coiled tubing. The coiled part of the tubing lies within the furnace so that the injected gas reaches the cell's temperature before entering the cell. Also a wire mesh is placed at the bottom of the cell to prevent any sand entering the system. Pressure gauges are placed to monitor supply pressure from the gas tank and inlet pressure to the cell. An error of $\pm 1\%$ span (500 psig) for the gauges is reported by the manufacturer (Wika industries).

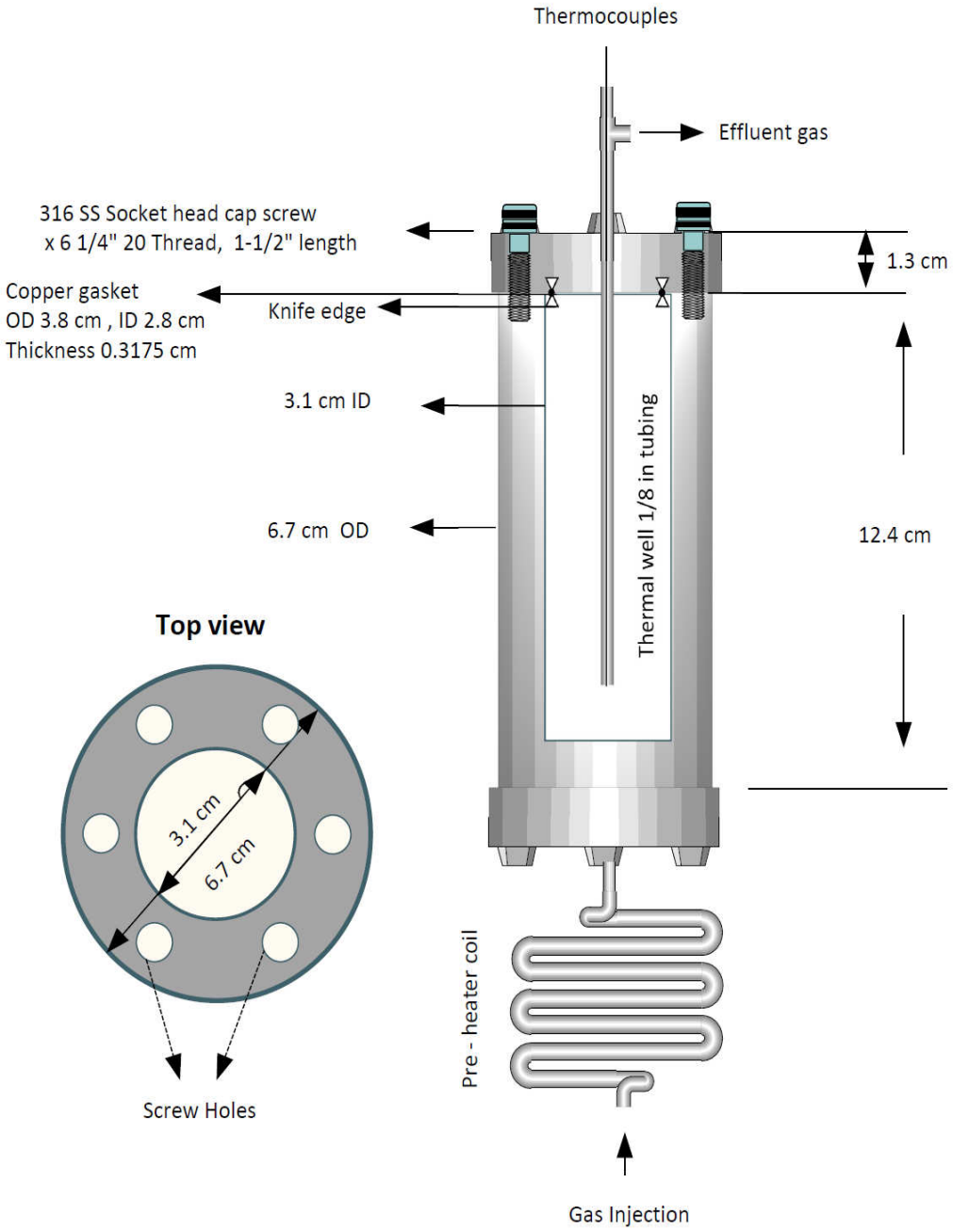


**Figure 3.2:** Schematic of the kinetic cell (Çınar, 2011).

### 3.2 Experimental Procedure

Kinetic experiments begin with sample preparation. This involves the homogenous mixing of a specified amount of sand (50g), 4ml water and 1.5g of crude oil. Porosity of sand is reported as 38% and permeability is undefined. Due to the viscous nature of the Bati Raman oil (12$^{o}$ API), the amount is obtained through trial and error methods. The amount of crude oil used is not too much to avoid temperature deviations from the pre-programmed temperature linear variation and also just enough to produce acceptable amount of effluent gas to be detected by the modules of the gas analyzer.

A small wire mesh is usually placed at the bottom of the kinetic cell to avoid sand from escaping through the coil used for gas injection. Dry sand is also filled at the bottom section of the kinetic cell to serve as a diffuser. After homogenous mixing of the sample is achieved, it is packed into a kinetic cell and screws are tightened.

Leak testing is conducted using nitrogen gas with the cell placed in a water bath to ensure the kinetic cell is fully pressure sealed. The experiment is conducted in a leak-free environment to avoid the effluent gas measurements from being compromised. After leak test is passed, the kinetic cell is placed in the electric furnace and connected to the filter system.

This three-stage filter system is placed to remove contaminants, which are contained in the effluent gas coming out of the kinetic cell from entering the gas analyzer. The filter is basically filled with two different mesh size sands namely fine and course sand. Condensing liquids in the effluent gas are also trapped in the liquid trap. To begin the kinetic cell experiment, the heating rate is changed to the desired time and all recording programs for gas and temperature opened from the mother computer. Air is injected at 2 standard liters per minute (SLPM) rate from the air tank.

The experiment begins with the initiation of temperature controller. Backpressures of 100, 150, 200 and 250 psig were used in all experiments. The kinetic cell experiment is fully automated and does not require any human effort during the experiments.

### 3.3 Experimental Samples And Pressures Used

The sand sample used for all experiments were obtained from Alacağızı area. Table 3.2 shows the general chemical composition of the Alacağızı sand sample. The reservoir rock was crushed and sieved into sizes of 350 microns. After sample sieving, the resulting sand was placed in the oven overnight to remove any contaminants as possible. Each experimental set consisted of five experiments conducted at different rates (1.62 K/min, 1.70 K/min, 1.90 K/min, 2.20 K/min, 2.40 K/min) and repeated at different pressures of 100, 150, 200 and 250 psig. Temperature target for all experiments was 650ºC (923.15 K).

**Table 3.2:** General Chemical Composition of Alacağızı Sand.

| Chemical | Percent Composition |
|---|---|
| $SiO_2$ | 98.10 |
| $Al_2O_3$ | 0.54 |
| $Fe_2O_3$ | 0.65 |
| $TiO_2$ | 0.02 |
| CaO | 0.10 |
| MgO | 0.09 |
| $Na_2O$ | 0.01 |
| $K_2O$ | 0.09 |
| $Cr_2O_3$ | 0.01 |
| MnO | <0.01 |
| $P_2O_5$ | 0.018 |
| SrO | <0.01 |
| BaO | <0.01 |

## 4. EXPERIMENTAL DATA AND ANALYSIS METHODS

Kinetic experiments were conducted using backpressures of 100, 150, 200 and 250 psig. The activation energy for each experiment is obtained using the conventional approach described by Fassihi (1981) and isoconversional analysis described by Friedman (1996) and adapted by Çinar (2011) to interpretate his RTO experiments.

### 4.1 Conventional Methods

Various conventional studies in the literature assume crude oil oxidation kinetics as a global (single step) reaction;

$$Fuel + O_2 \rightarrow CO_2 + CO + H_2O \quad \textbf{(4.1)}$$

The rate of Equation 4.1 is found by assuming an Arrhenius type rate constant;

$$R_c = -\frac{dC_{fuel}}{dt} = KP_{O_2}^{a} C_{fuel}^{b} \quad \textbf{(4.2)}$$

The rate constant, *K* is usually a function of temperature and follow the Arrhenius law (Carberry, 1976 ; Smith, 1970).

$$K(T) = A\exp\left(-\frac{E}{RT}\right) \quad \textbf{(4.3)}$$

If the order of reaction with respect to oxygen is assumed as unity ($a$=1) then the reaction order of carbon, b is evaluated from Equation 4.2 by taking logarithm on both sides to obtain Equation 4.4;

$$\log\left(-\frac{dC_{fuel}/dt}{P_{O_2}}\right) = b\log C_{fuel} + \log K \quad \textbf{(4.4)}$$

The activation energy ($E$), which represents the energy barrier to be overcome by molecules for a reaction to occur, can be obtained through Equation 4.5.

$$\ln K = \ln A - \left(\frac{E}{RT}\right) \quad \textbf{(4.5)}$$

Equations 4.1 to 4.5 form the basis of early kinetic studies performed by various investigators within the literature (Bousaid and Ramey, 1968; Burger and Suhuquet, 1972; Mamora, 1993).

### 4.1.1 Fassihi's oxidation model

Fassihi (1981) proposed an oxidation reaction model in his non-isothermal kinetic studies. In this reaction model, reaction kinetics are grouped into three regions namely as low temperature oxidation (LTO), middle temperature reaction (MTR), and high temperature oxidation (HTO). The equations below formulate the basis for the calculation of activation energy in the HTO region, which is of interest in this thesis work. Further equations on the LTO and MTR can be referenced from Fassihi's PhD thesis work.

The change in oxygen concentration, $\Delta Co_2$ during the kinetic experiment can be calculated from Equation 4.6 as;

$$\Delta Co_2 = O_2 - \frac{N_{2i}O_2}{N_{2p}} = \frac{O_{2i}(1 - CO_2 - CO) - O_2}{1 - CO_2 - CO - O_2} \quad \textbf{(4.6)}$$

The subscripts, *i* and *p* represents the injected and produced gas concentrations.

The rate of oxygen consumption per unit volume is given as;

$$\frac{q\Delta C_{O_2}}{A_c L} = AP_{O_2}^a C_{fuel}^b \exp\left(-\frac{E}{RT}\right) \quad \textbf{(4.7)}$$

Here $q$ represents the volumetric flow rate (lt/min), $A_c$ the cross-sectional area ($cm^2$) and L is the length (cm) of the sand mix in the kinetic cell.

It is assumed that the rate of oxygen consumption is proportional to the rate of decrease of fuel as;

$$\frac{q\Delta C_{O_2}}{A_c L} = -v\frac{dC_{fuel}}{dt} \quad \textbf{(4.8)}$$

$v$ is a proportionality factor given by Fassihi (1981) as equal to the amount of oxygen in moles that reacts with 1g of fuel. $v$ can be evaluated as shown in Equation 4.9;

$$v = \frac{q}{A_c L} \frac{\int_t^\infty \Delta C_{O_2} dt}{\int_t^\infty (C_c + C_{H_2}) dt} \quad \textbf{(4.9)}$$

$C_c$ and $C_{H_2}$ are the instantaneous concentration of carbon and hydrogen burned. The rate of oxygen consumption at any time can be obtained by combining Equations 4.7 and 4.8;

$$\frac{q\Delta C_{O_2}}{A_c L} = AP_{O_2}^a C_{fuel}^b \left(-\frac{E}{RT}\right) = -v\frac{dC_{fuel}}{dt} \quad \textbf{(4.10)}$$

Integration of Equation 4.10 from time *t* to time infinity yields;

$$vC_{fuel}(t) = \int_t^\infty \frac{\Delta C_{O_2}}{A_c L} dt' \quad \textbf{(4.11)}$$

From Equation 4.7, $C_{fuel}$ = 0 at t=∞. We can then get a term for $C_{fuel}^b$ as:

$$C_{fuel}^b(t) = \frac{q}{A_c L} \frac{1}{AP_{O_2}^a \exp\left(-\frac{E}{RT}\right)} \quad \textbf{(4.12)}$$

If we substitute Equation 4.12 into Equation 4.11, we obtain the following expression:

$$\frac{\Delta C_{O_2}}{\left(\int_t^\infty \Delta C_{O_2} dt'\right)^b} = \beta' \exp\left(-\frac{E}{RT}\right) \quad \textbf{(4.13)}$$

$$\beta' = \left(\frac{q}{A_c L}\right)^{b-1} \frac{AP_{O_2}^a}{v^b} \quad \textbf{(4.14)}$$

The left – hand side of Equation 4.13 is evaluated through integration of the oxygen consumption by using either Trapezoidal or Simpson's rule with respect to time $\Delta C_{O_2} = f(t)$. The values obtained can be plotted against 1/T to obtain the slope as *–E/RT* and $\beta'$ as the intercept. Activation (*E)* obtained here is in the HTO region. The left-hand side of Equation 4.13 is termed as the "Relative Reaction Rate (RRR)" - (Fassihi, 1981).

### 4.2 Isoconversional Approach

For the combustion of crude oil, Equation 4.2 is the simplest way of representing the reaction rate of fuel. However, Semenov (1935) disputes the overly simple representation of fuel oxidation given by Equation 4.1. The isoconversional analysis method provides a way to bypass the complex and unknown reaction models involved in crude oil combustion. Equation 4.2 can be written in a simple form as a function of temperature and concentration, *C*.

$$-\frac{dC}{dt} = K(T)\,f(C) \qquad \textbf{(4.15)}$$

*K(T)* is the rate constant and *f((C)* is the reaction model.

$$K(T) = A\exp\left(-\frac{E}{RT}\right) \qquad \textbf{(4.16)}$$

The isoconversional principle states that, the reaction rate at a constant extent of conversion (X) is only a function of temperature (Friedman, 1964). Under this assumption, it implies that at the same conversion, the value of *f(C)* in Equation 4.15 is equal irrespective of the temperature. We can substitute Equation 4.16 into Equation 4.15 and rearrange in terms of conversion *X*, which can be estimated from oxygen consumption to obtain the following expression:

$$\frac{dX}{dt} = Ae^{-E/RT}\,f(X) \qquad \textbf{(4.17)}$$

Taking natural logarithm of both sides of Equation 4.17 gives the following expression:

$$\ln\left(\frac{dX}{dt}\right) = \ln A + \ln\left[f(X)\right] - \frac{E}{RT} \qquad \textbf{(4.18)}$$

Equation 4.18 is known in the literature as the Friedman method or differential isoconversional method. It forms the basis of all isoconversional methods within the literature. If 3-5 series of experiments are conducted at different heating rates, a plot of left-hand side (LHS) vs 1/T gives a slope of –E/R from which activation energy (E) can be obtained without assuming/determining any particular kinetic model as the use of Equation 4.2 in conventional methods. In *A* and In *f(X)* become constants on the intercept which are same for different heating rates.

### 4.2.1 Equations for isoconversional analysis

Çınar (2011) develops the following equations for the kinetic cell experimental design. The kinetic cell can be assumed as a reactor in the sense that, it is filled with oil-sand-water mixture and a linear heating rate is imposed with air injected at a constant pressure (steady-state). During the duration of the experiment, carbon oxides, water and other hydrocaarbon are continuously produced. If we assume no gravity effects, laminar flow and no radial variation for concentration, velocity and temperature as well as no spatial variation for the reaction rate in view of the large air rate then we can write a mass balance for the kinetic cell as:

$$Flow_{in} - Flow_{out} + Generation\ \ Term = Accumulation\ \ Term \qquad \textbf{(4.19)}$$

Mathematically, this can be expressed as :

$$F_{jo} - F_j + \int_v r_j dV = \frac{dN_j}{dt} \qquad \textbf{(4.20)}$$

Where:

$F_{jo}$ molar flow rate of species j into the system, mol/min

$F_j$ is molar flow rate of species j out of the system, mol/min

$r_j$ is the generation term (sink)

$dN_j/dt$ is the accumulation term

Molar flow rate, F is related to concentration, C and volumetric flow rate, q as:

$$F = Cq = \left(\frac{mol}{lt}\right) \times \left(\frac{lt}{\min}\right) = \frac{mol}{\min} \qquad \textbf{(4.21)}$$

After the integral in Equation 4.20 is taken the mole balance becomes:

$$F_{jo} - F_j + r_j V = \frac{dN_j}{dt} \qquad \textbf{(4.22)}$$

If we consider the addition of air (oxygen) from the tank to the kinetic cell at a constant pressure and assume that there is a perfect mixing of fuel and air, then the accumulation term can be neglected from Equation 4.22 and written as:

$$\frac{F_{O_2 o} - F_{O_2}}{V} = -r_{O_2} \qquad \textbf{(4.23)}$$

We can also write a mass balance for the fuel noting that there is no in and out flow of fuel :

$$r_{fuel} = \frac{dC_{fuel}}{dt} \tag{4.24}$$

If we define $\alpha$ as the number of moles of oxygen consumed per mole of fuel that reacts then we can relate the rates of disappearance of fuel and oxygen in a relation :

$$r_{fuel} = \frac{r_{O_2}}{\alpha} \tag{4.25}$$

In the RTO experiments with effluent gas analysis method, the oxygen consumed is measured and not the weight of the fuel. Equations 4.23 and 4.24 helps to avoid any discrepancies caused by phase changes. We can substitute Equation 4.23 into Equation 4.25 to obtain a new term for the rate of disappearance of fuel as:

$$\frac{-dC_{fuel}}{dt} = \frac{F_{O_2} - F_{O_2}}{V} \frac{1}{\alpha} \tag{4.26}$$

If Equation 4.26 is integrated from time zero to any time t and rearranged in terms of conversion we obtain :

$$X_{fuel}(t) = \frac{1}{C_{fuel_o}} \frac{1}{\alpha V} \int_0^t (F_{O_{2,o}} - F_{O_2}) dt \tag{4.27}$$

Conversion,

$$X_{fuel} = 1 - \frac{C_{fuel}(t)}{C_{fuel}(t=0)} \tag{4.28}$$

Without an extensive compositional analysis, initial molecular weight and concentration of fuel is difficult to estimate (Çınar, 2011).Since it is known that as time goes to infinity conversion, $X_{fuel}$ goes to unity and all fuel is consumed, then Equation 4.27 becomes:

$$\frac{1}{C_{fo}} \frac{1}{\alpha V} = \frac{1}{\int_0^\infty (F_{O_2,o} - F_{O_2}) dt} \tag{4.29}$$

We can then write conversion as :

$$X_{fuel} = \frac{\int_0^t (F_{O_{2o}} - F_{O_2})dt}{\int_0^\infty (F_{O_{2o}} - F_{O_2})dt} \quad \textbf{(4.30)}$$

Finally if we substitute Equation 4.21 into Equation 4.30, conversion can be written in terms of molar concentration, C as:

$$X_{fuel} = \frac{\int_0^t (C_{O_{2o}} - C_{O_2})dt}{\int_0^\infty (C_{O_{2o}} - C_{O_2})dt} \quad \textbf{(4.31)}$$

To apply the isoconversional analysis method, Equations 4.18 and 4.31 are used alongside recorded temperature measurements.

### 4.3 Results and Discussions

The results obtained from the analysis methods are presented in the section 4.3.1 for Fassihi's method and section 4.3.2 for isoconversional method. A matlab program using Stormy (2013) as a guide was written to help in the handling of large data output from the gas analyzer and the temperature recorder.

#### 4.3.1 Fassihi analysis

Plots obtained for different heating rates at 150 psig are given in Figures 4.1 through 4.5 to illustrate the analysis procedure for Fassihi's method in the HTO region. In all the figures: (a) represents the gas composition curves, (b) represents the programmed temperature profile, (c) represents the plot of relative reaction rate vs inverse of temperature and (d) is the HTO linear decomposition straight line obtained from (c). Table 4.1 summarizes the activation energy values estimated for all heating rates at 100 , 150 , 200 , and 250 psig.

The gas composition curves (a) obatined for all heating rates clearly shows the LTO, the first peak (smaller), MTR, the negative region ('valley of Death') where oxygen consumption decreases even as temperature increases. The second peak (higher) HTO region represents the combustion region where the injected oxygen reacts with the deposited coke to sustain the heat at the combustion front.

It is not necessary that the LTO peak should always be smaller than the HTO peak for heavy crude oils as observed in Figures 4.1 through 4.5. Bardon and Gadelle (1977) reported that for a French oil the LTO peak was much higher than the HTO peak. The height of the LTO and HTO gives some information about the reactivity of the oil being used for analysis. According to Fassihi et al. (1984a) very high HTO peak than the LTO peak indicates the propensity of the oil to deposit coke on the rock matrix whereas a much higher LTO peak than the HTO indicates the reactivity of the oil with oxygen at low temperature conditions.

It must be noted that an oil that deposits too much coke on the rock matrix increases the air requirements for in situ combustion operation, whereas an oil that deposits a small amount of coke on the rock matrix does not provide enough fuel to sustain the fire front for the combustion process.

It can be observed from gas composition plots that during the LTO, oxygen is consumed to produce a low amount of carbon dioxide and carbon monoxides. It seems that the total amount of produced carbon oxides in the LTO region does not equal the amount of oxygen consumed. This clearly indicates that consumed oxygen is used in other reactions. However, in the HTO regions the produced carbon oxides are almost equal to the consumed oxygen and good indication of complete combustion. From Table 4.1. it is realized that estimated activation energy values generally decrease with increasing heating rate.

The programmed temperature recorder shows three deviations, first is at 350K (76.85$^{o}$C) which is attributed to the evaporation of water from the kinetic reactor and second in the LTO region and third in the HTO region those. Deviations in LTO and HTO regions are direct results of exothermic reactions. Figures 4.1 – 4.5 show the plots used in the activation energy evaluation by the use of Fassihi's analysis procedure for the HTO region for the experiments conducted at 150 psig.

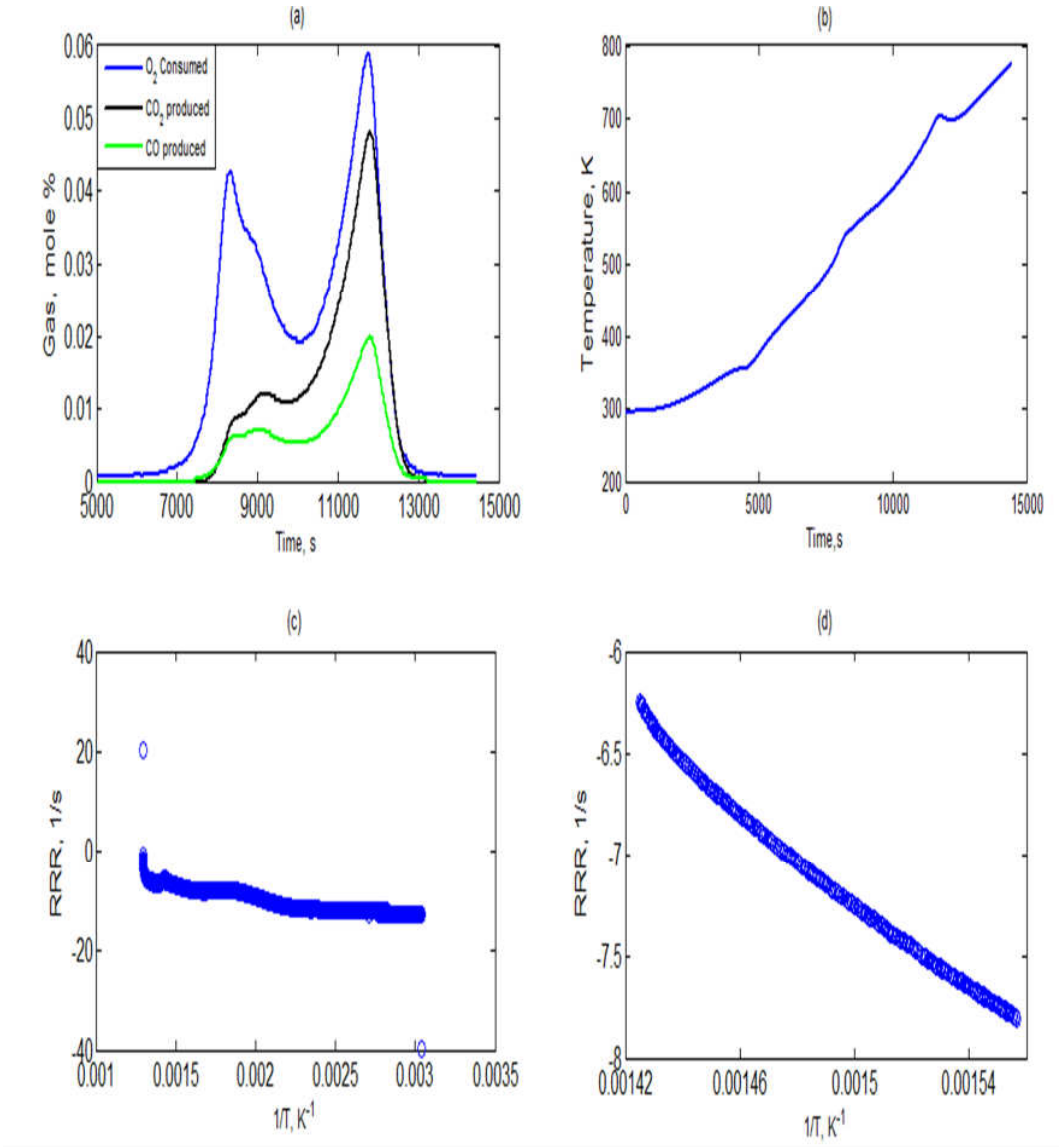


**Figure 4.1:** Kinetic plots for heating rate of 2.40 K/min (150 psig).
(a) Gas composition curves (b) Programmed temperature profile (c) Relative reaction rate (RRR) vs inverse of temperature, 1/T (d) Linear decomposition straight line obtained from HTO region of (c).

An activation energy value of 94000 J/mol was estimated for the HTO region.

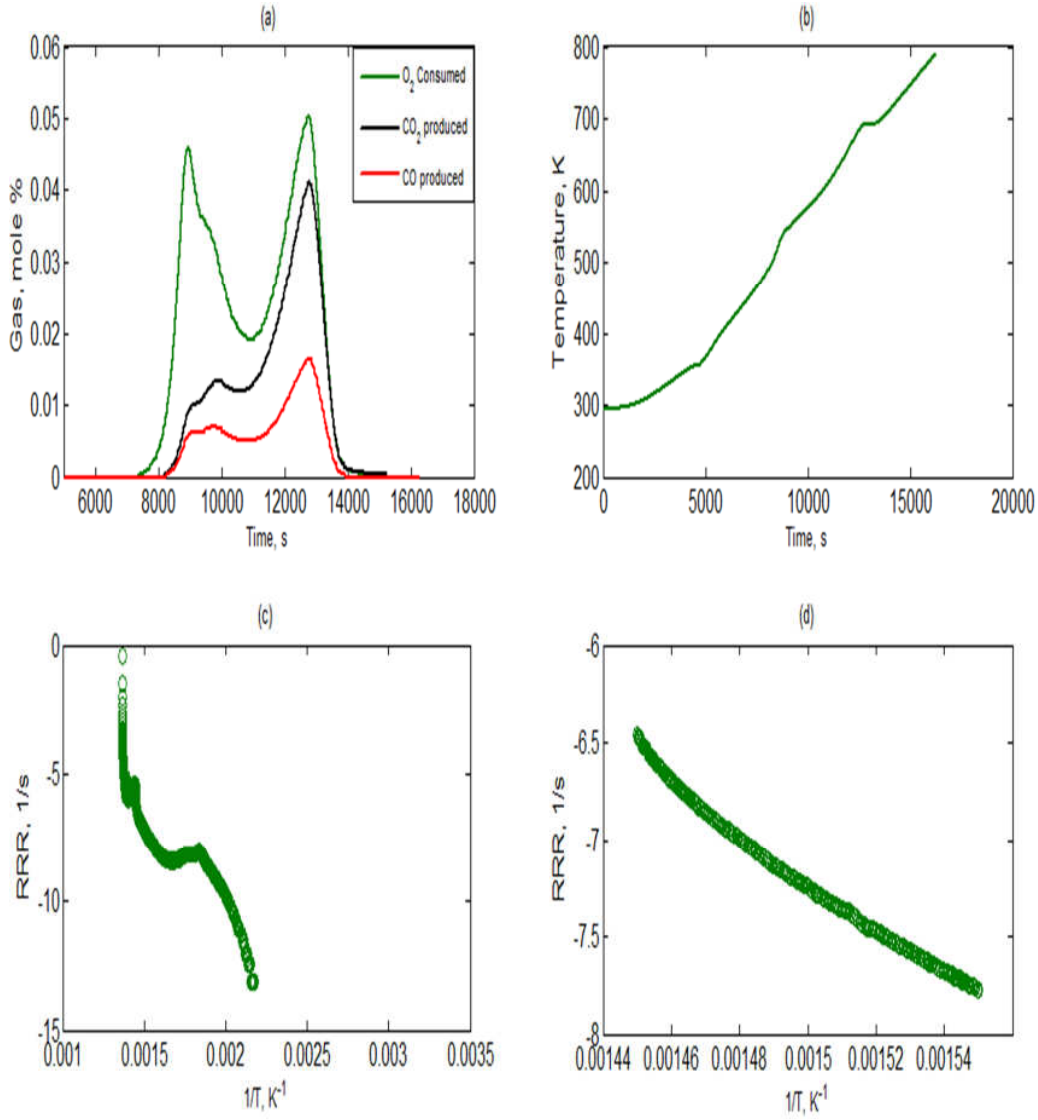


**Figure 4.2:** Kinetic plots for heating rate of 2.20 K/min (150 psig).
(a) Gas composition curves (b) Programmed temperature profile (c) Relative reaction rate (RRR) vs inverse of temperature, 1/T (d) Linear decomposition straight line obtained from HTO region of (c).

Activation energy value estimated in the HTO region is 104000 J/mol.

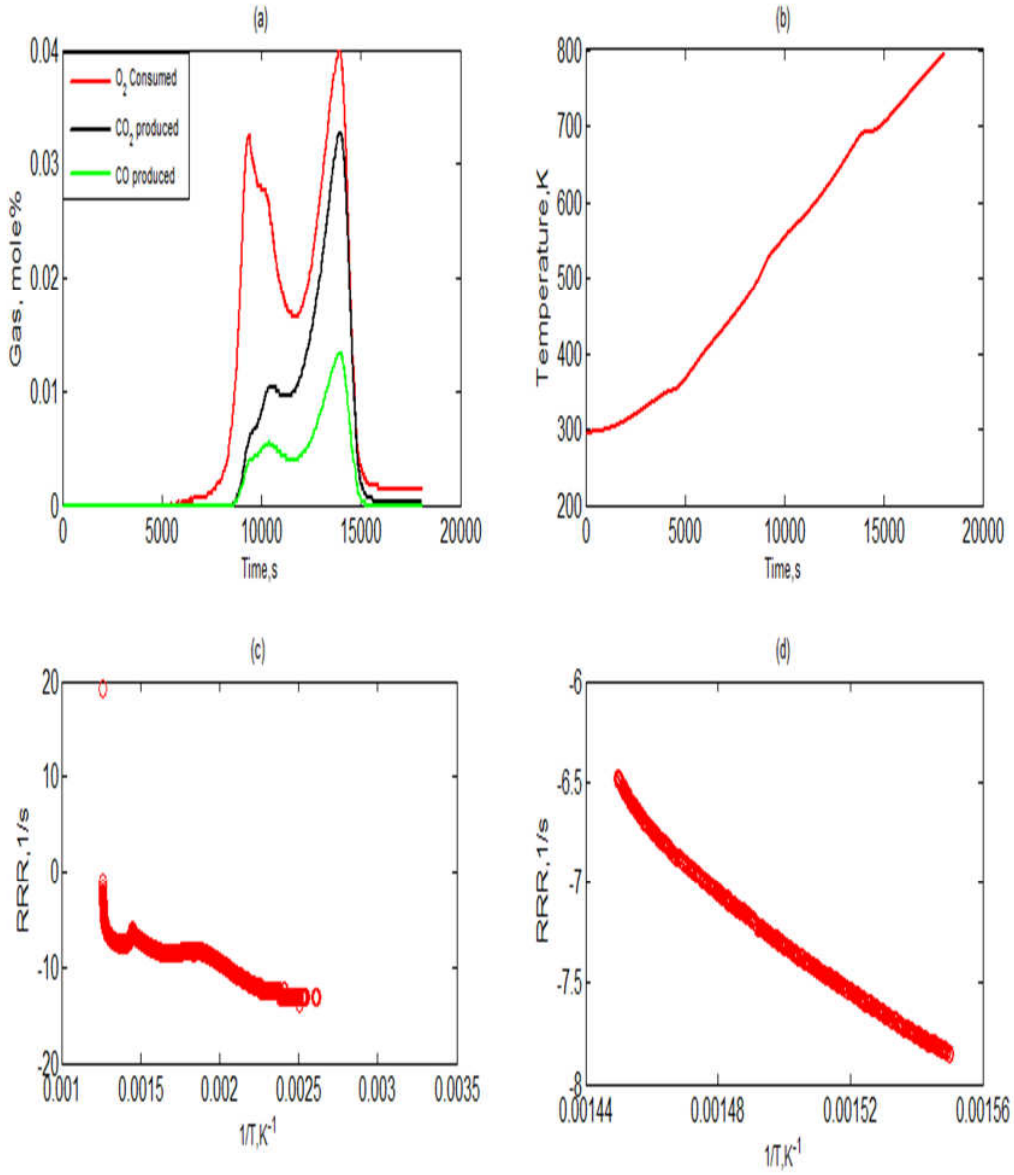


**Figure 4.3:** Kinetic plots for heating rate of 1.90 K/min (150 psig).
(a) Gas composition curves (b) Programmed temperature profile (c) Relative reaction rate (RRR) vs inverse of temperature, 1/T (d) Linear decomposition straight line obtained from HTO region of (c).

HTO activation energy obtained is 109000 J/mol.

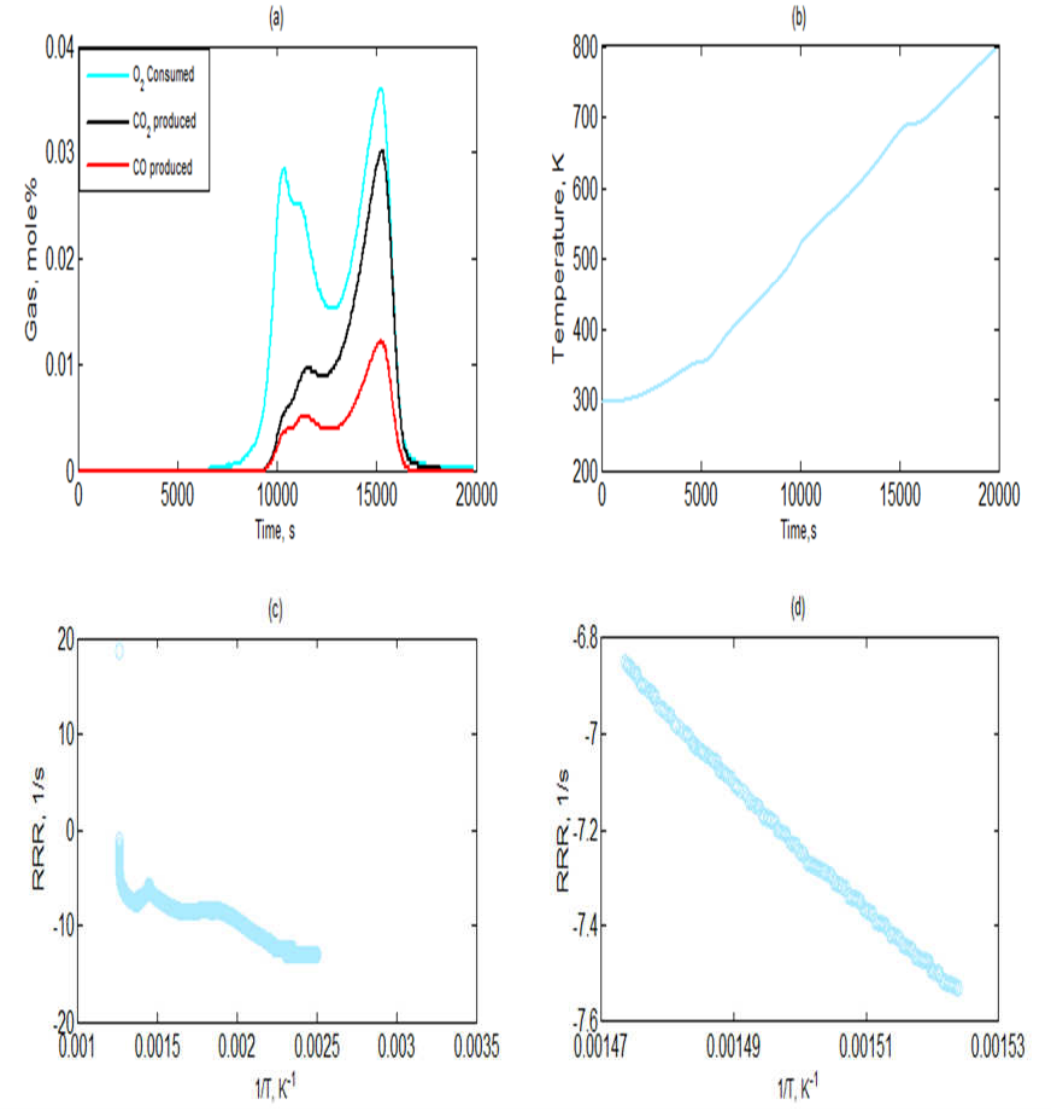


**Figure 4.4:** Kinetic plots for heating rate of 1.70 K/min (150 psig).
(a) Gas composition curves (b) Programmed temperature profile (c) Relative reaction rate (RRR) vs inverse of temperature, 1/T (d) Linear decomposition straight line obtained from HTO region of (c).

The HTO activation energy value estimated is 112000 J/mol.

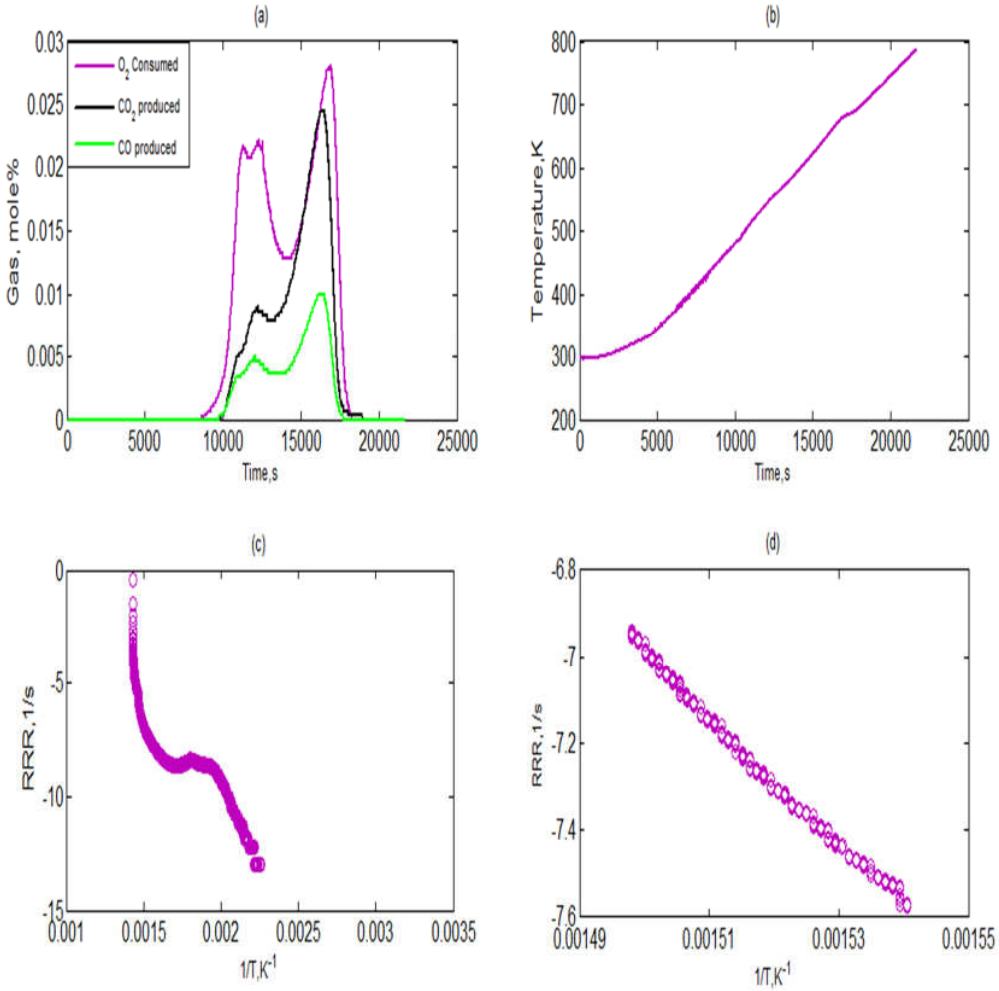


**Figure 4.5:** Kinetic plots for heating rate of 1.62 K/min (150 psig).

(a) Gas composition curves (b) Programmed temperature profile (c) Relative reaction rate (RRR) vs inverse of temperature , 1/T (d) Linear decomposition straight line obtained from HTO region of (c).

An activation energy value of 120000 J/mol is evaluated in the HTO region.

Table 4.1 summarizes the activation energies obtained for the various heating rates in all operating pressures using the Fassihi (1981) method of analysis.

**Table 4.1:** HTO activation energy evaluated with Fassihi's method.

| Pressure psi | 2.40 K/min | 2.20 K/min | 1.90 K/min | 1.70 K/min | 1.62 K/min | Average J/mol |
|---|---|---|---|---|---|---|
| 100 | - | 82000 | 85000 | 87000 | 89000 | 87000 |
| 150 | 94000 | 104000 | 109000 | 112000 | 120000 | 108000 |
| 200 | 94000 | 110000 | 120000 | 120000 | 130000 | 115000 |
| 250 | 120000 | 133000 | 140000 | 150000 | 150000 | 140000 |

### 4.3.2 Results for isoconversional analysis

Experiments conducted at different pressures of air injection with the same sand sample were analyzed with the isoconversional analysis. Each pressure RTO experiment was conducted at five different heating rates. For each set of heating rates, isoconversional analysis was applied to $O_2$, $CO_2$, and CO data. Results are summarized for each pressure case in the following sections.

#### 4.3.2.1 Experiments at 100 psig

Isoconversional analysis was applied to consumed oxygen, produced carbon dioxides and carbon monoxides measured in all five heating rates. The aim is to generate isoconversionl fingerprints and estimate the activation energy for Bati Raman crude oil. Figure 4.6 gives the set of oxygen data along with temperature measurements used for obtaining the oxygen fingerprint in Figure 4.7.

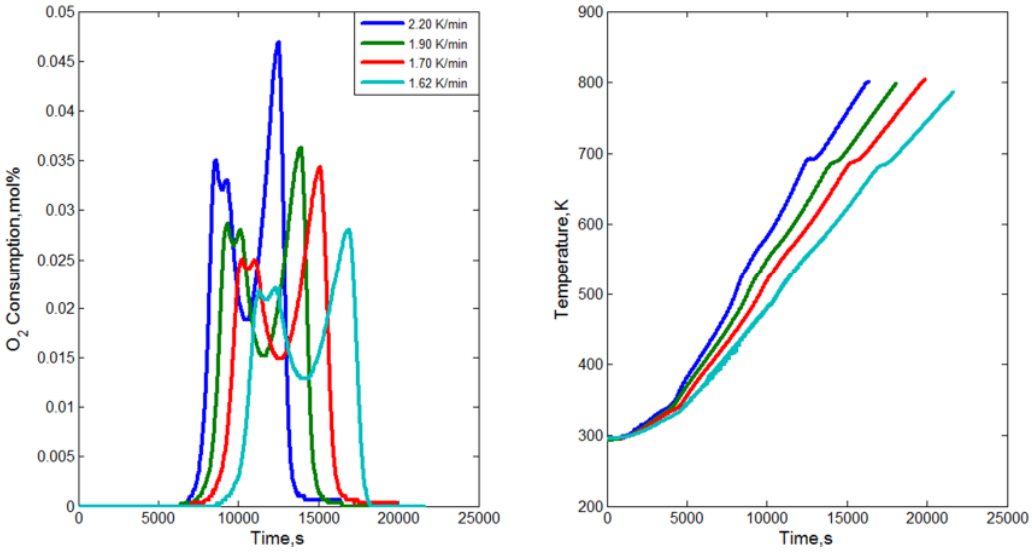


**Figure 4.6:** Oxygen consumption (left) and temperature profile (right) at 100 psig.

Temperature data for 2.4 K/min were not consistent with the other recorded temperature and therefore it was ommitted alongside its oxygen consumption from the analysis: The general trends observed in other experiments were not observed in aformentioned one. This experiment was repeated several times, however, a meaningful set of data was not obtained because of operational problems. In Figure 4.6, it is seen clearly that peak oxygen consumption increases with increasing heating rate in both HTO and LTO regions. The temperature recorder was programmed to take measurements at a frequency of 1K/s.

There is an observed deviation at around 350K, this can be attributed to the vaporisation of water from the sample mixture in the kinetic cell. A hump is seen in the middle section of the temperature profile around 550K. This can be evidence of LTO reactions. Finally a major departure from the programmed temperature recorder occurs at 680K indicating HTO reactions. As stated earlier, using Equation 4.18 and 4.31 alongside recorded oxygen and temperature measurements the fingerprint for oxygen is obtained in Figure 4.7.

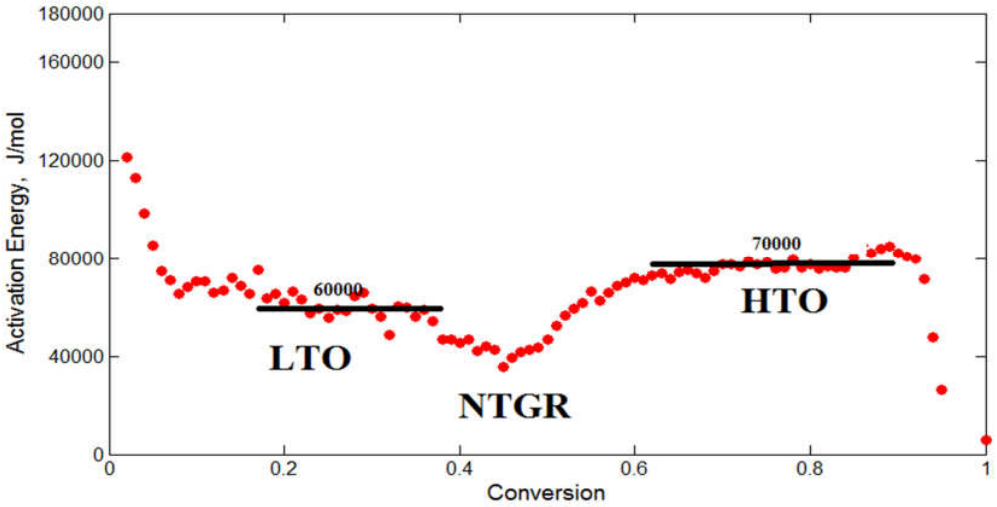


**Figure 4.7:** Isoconversional fingerprint for oxygen at 100 psig

The isoconversional fingerprint above shows the LTO (conversion 0.1-0.3), NTGR (conversion 0.3-0.6), and HTO (conversion 0.6-0.9), regions. We can estimate activation energy values for different regions from the stabilized activation energy values developed. These stabilized values are indicative of dominant reactions that are occuring in each respective region. Two stabilized regions are observed in Figure 4.7; LTO and the HTO region. HTO activation energy is estimated at around 70000 J/mol. In the LTO region stabilized values are around 60000 J/mol.

Then we apply isoconversional analysis method to carbon oxides produced from oxygen consumption. The data set of produced carbon oxides at 100 psig are shown in Figure 4.8. From Figure 4.8, it can be observed that, more carbon dioxides are produced than carbon monoxides at each heating rate. Amount of carbon dioxides produced at each heating rate is almost doubled that of carbon monoxides.

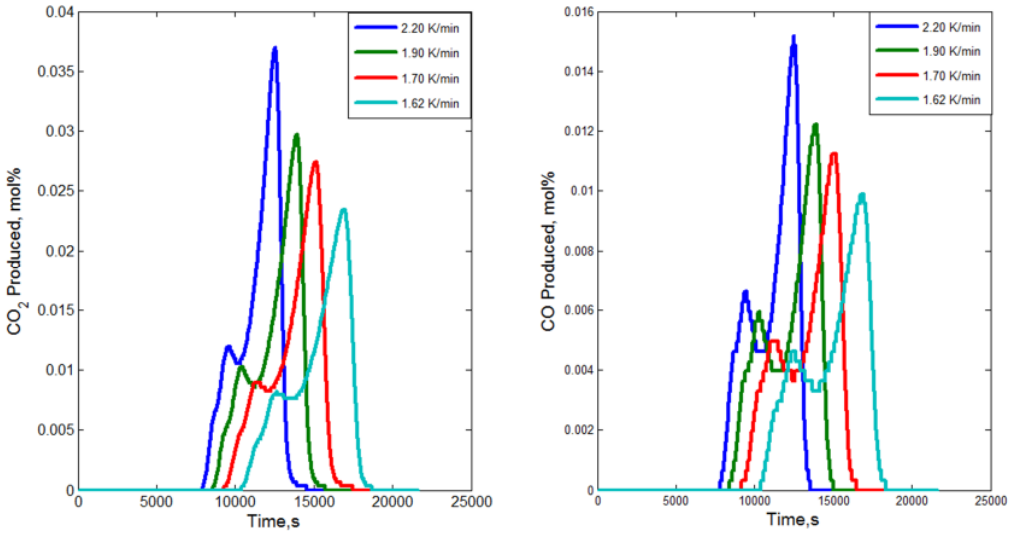


**Figure 4.8:** Produced carbon dioxides (left) and carbon monoxides (right) at 100 psig.

Using data obtained in Figure 4.8 and recorded temperature in Figure 4.6, isoconversional fingerprints for carbon oxides were generated. In Figure 4.9, the combined fingerprints for oxygen, carbon dioxide and carbon monoxide are shown.

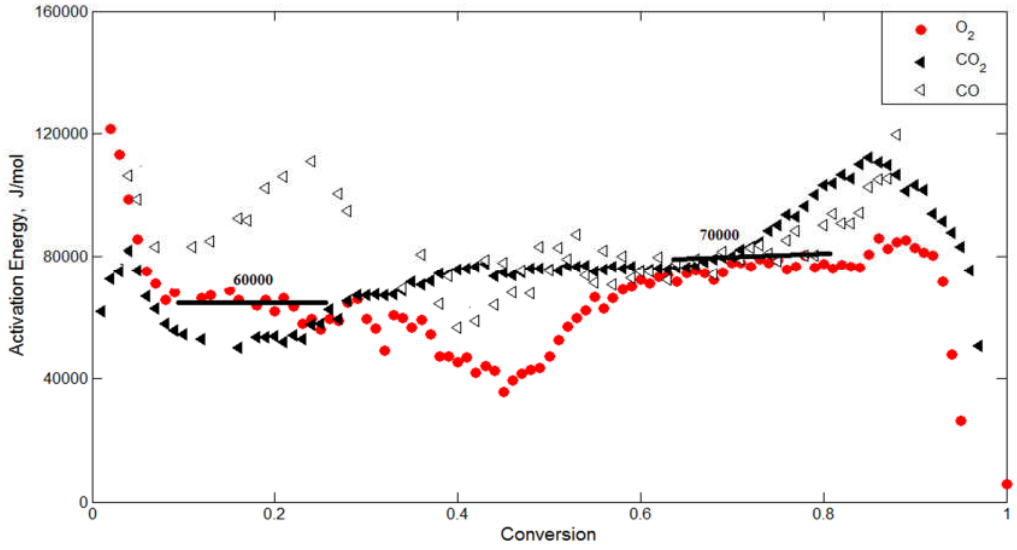


**Figure 4.9:** Combined isoconversional fingerprints for oxygen and produced carbon oxides at 100 psig.

The fingerprints obtained for the produced carbon oxides do not fit that of oxygen in the NTGR as seen in Figure 4.9. Also the NTGR for the carbon oxides fingerprints appear to be shifted to the left of the NTGR of oxygen fingerprint. This is an expected behaviour because curves are based on conversion of different species; time dependence of convergence would be different for different components.

One other observation regards oxygen consumption. A mole balance indicates that not all the oxygen converted are produced as carbon oxides. Remaining oxygen takes part in oxygen addition reactions. Therefore by applying a mole balance, we can find the amount of oxygen taking part in oxygen addition reactions to generate its isoconversional fingerprint. For generation of one mole of carbon dioxide one mole of oxygen gas is needed. Similarly, one mole of oxygen gas could generate two moles of carbon monoxide. If $O_2$ represents total moles of oxygen consumed and $CO_2$ and CO represernt total moles of carbon dioxide and carbon monoxide produced then $O_2$-$CO_2$-CO/2 would yield total moles of oxygen gas that takes part in oxygen addition. Data obtained for the oxygen addition reactions is shown in Figure 4.10.

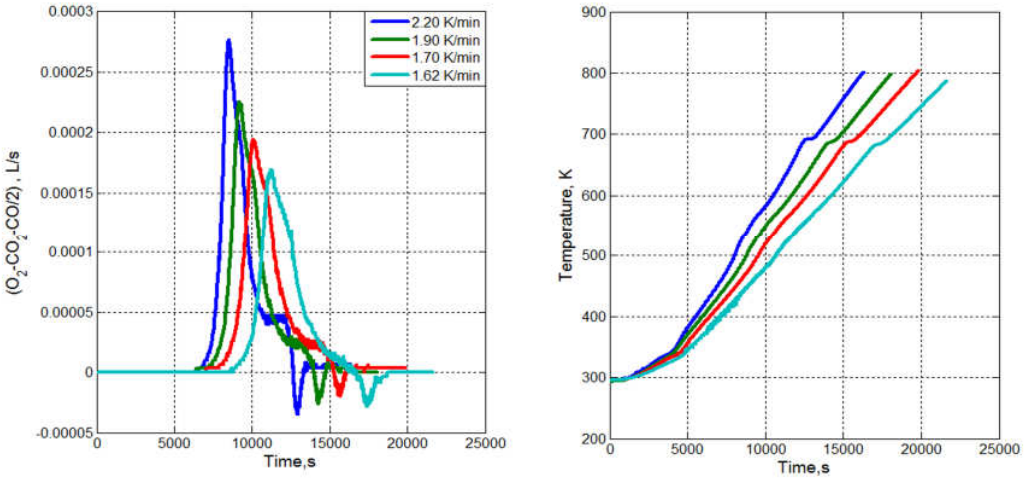


**Figure 4.10:** Oxygen addition (left) and temperature profile (right) at 100 psig.

The data set obtained in Figure 4.10, shows a negative consumption for all heating rates at later times. A possible explanation could be the oxygen atoms attached to carbon surface on the coke as oxygen functional groups. While coke burns, oxygen attached to the molecular structure of coke also are produced as carbon oxides. We regret that we cannot provide further experimental evidence to support the idea. Using the data set in Figure 4.10 along with temperature recording of Figure 4.7 the isoconversional procedure is applied and the fingerprint generated is shown in Figure 4.11.

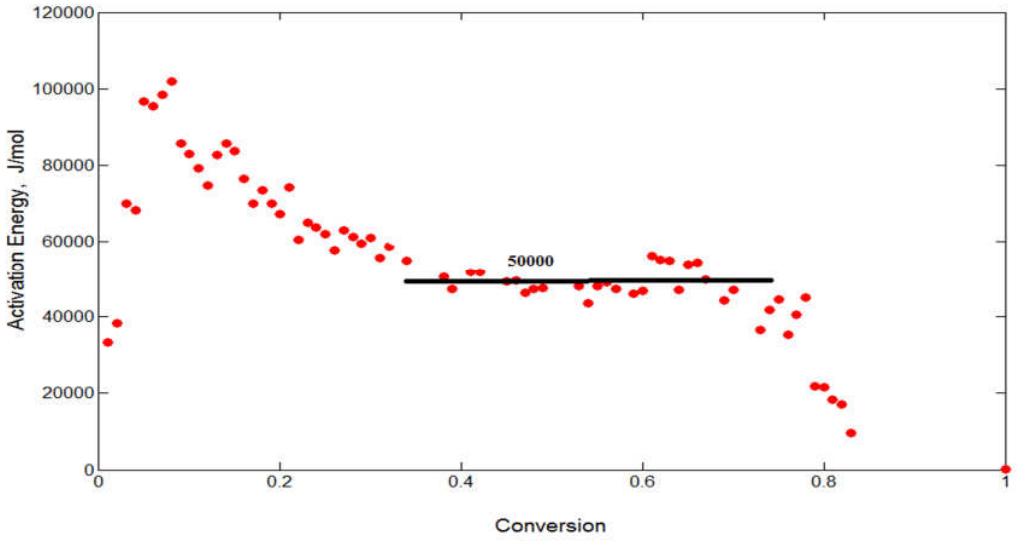


**Figure 4.11:** Isoconversional fingerprint for oxygen addition at 100 psig.

From Figure 4.11, LTO activation energy of 50000 J/mol is estimated for oxygen addition.

### 4.3.2.2 Experiments at 150 psig

Experiments were repeated at 150 psig to obtain isoconversional fingerprints and activation energies. Figure 4.12 shows the oxgyen and recorded temperature at various heating rates.

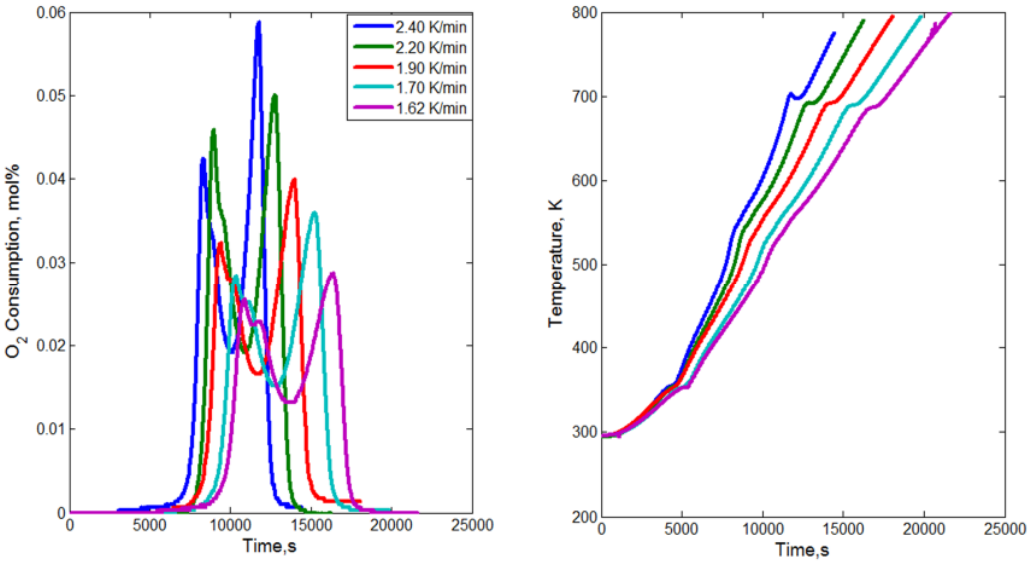


**Figure 4.12:** Oxygen consumption (left) and temperature profile (right) at 150 psig.

The oxygen data show a good consistency and an observation is made that higher heating rates have high oxygen peaks. Using the oxygen data along with recorded temperature, the isoconversional method is applied to obtain the fingerprint in Figure 4.13.

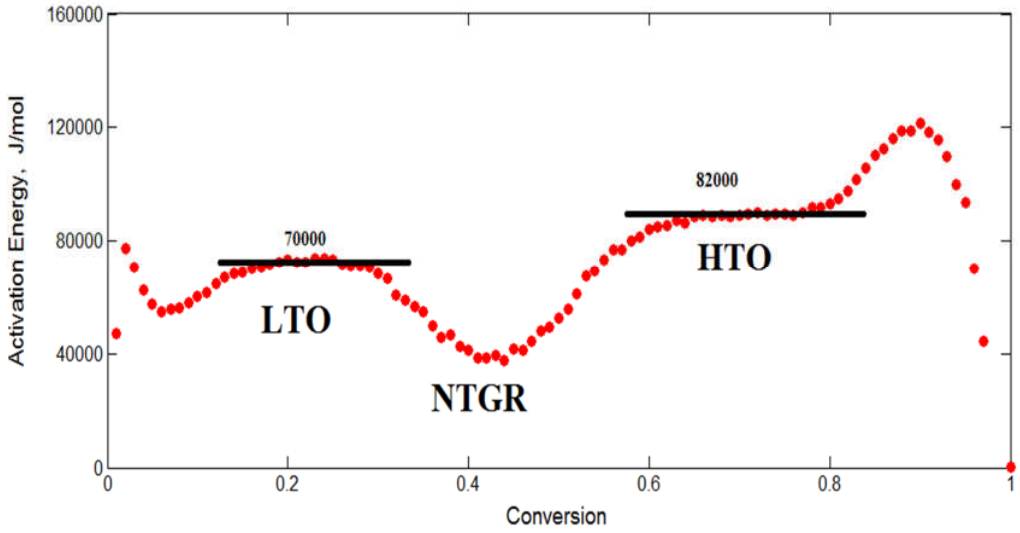


**Figure 4.13:** Isoconversional fingerprint for oxygen at 150 psig**.**

HTO activation energy is estimated around 82000 J/mol. The HTO activation energy for 150 psig is higher than that obtained for 100 psig which was estimated at 70000 J/mol. The produced carbon oxides data are also graphed in Figure 4.14.

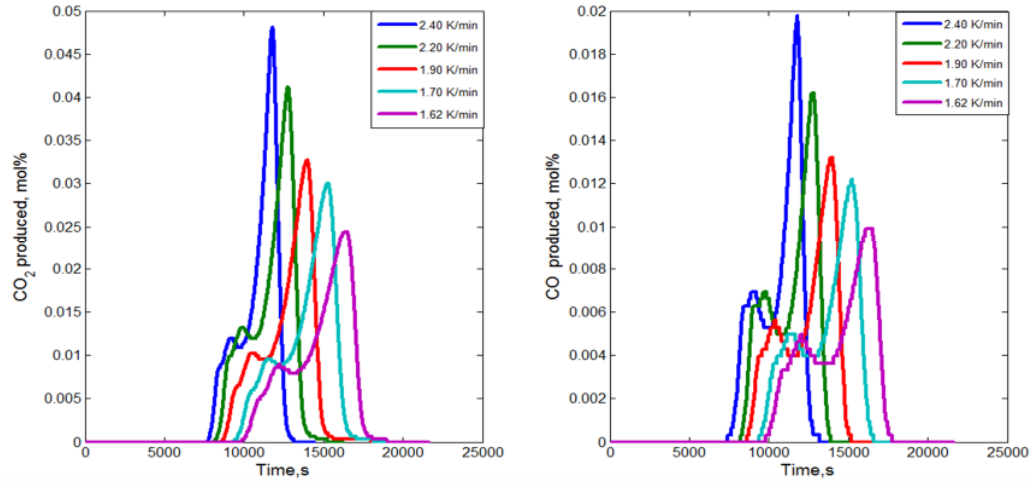


**Figure 4.14:** Produced carbon dioxide (left) and carbon monoxide (right) at 150 psig.

The produced carbon oxides data also show a good consistency and therefore the isoconversional method can be applied along with recorded temperature profile in Figure 4.12. The amounts of produced carbon dioxides are more than those of monoxides at each heating rates as seen in Figure 4.14 above. Also carbon dioxides produced at each heating rate are almost doubled that of carbon monoxides. Figure 4.15 shows the combined isoconversional fingerprint for oxygen, carbon dioxide and carbon monoxide at 150 psig.

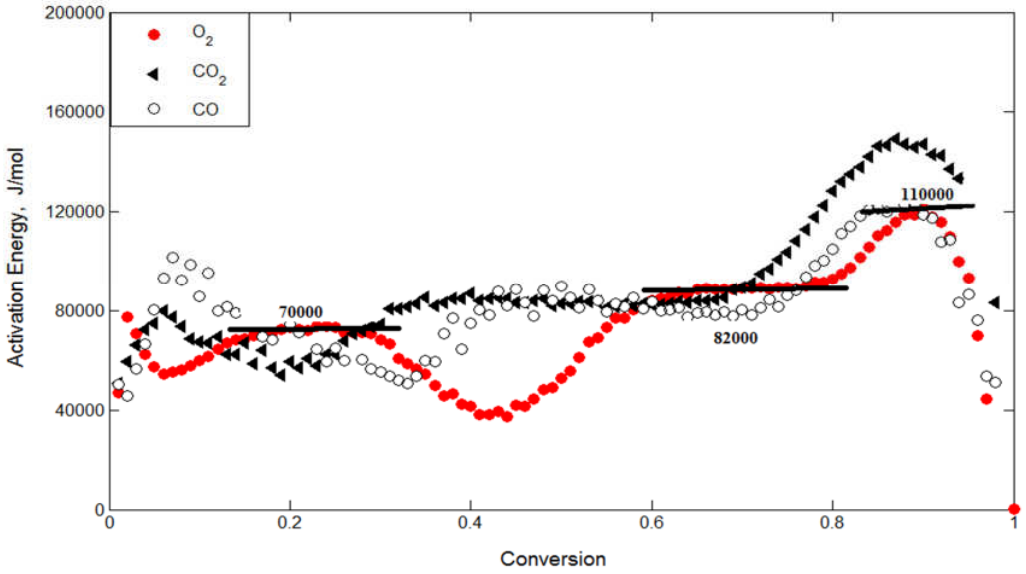


**Figure 4.15:** Combined isoconversional fingerprints for oxygen and produced carbon oxides at 150 psig.

It can be observed from Figure 4.15 that, NTGR for the produced carbon oxides fingerprints are shifted to the left of the NTGR of oxygen fingerprint. This phenomenom has already been discussed for 100 psig case and same reason is attributed to the 150 psig experiments. Also close proximity of activation energy values in the HTO region obtained for both carbon oxides and oxygen indicates that carbon oxides production and oxygen consumption are controlled by the same reaction having an activation energy of around 82000 J/mol. On the other hand in LTO region, there are more than one controlling reactions for oxygen consumption and carbon oxides production as isoconversional analysis do not yield the same value. Also the fingerprints indicate another controlling reaction with an activation energy of 110000 J/mol at large conversions. The amounts of oxygen not used in the production of carbon oxides is estimated at each heating rate and graphed along with recorded temperature data in Figure 4.16.

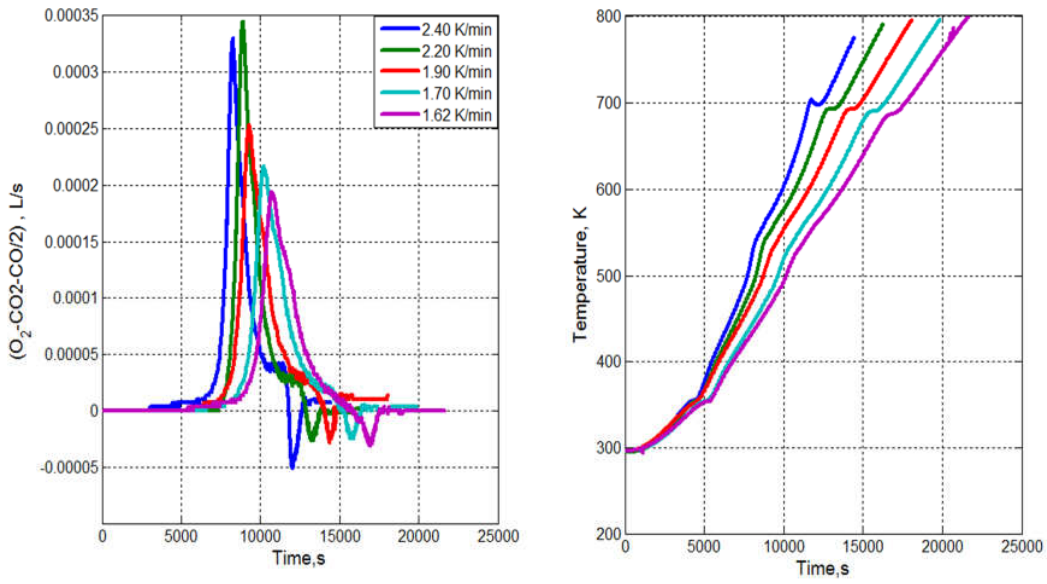


**Figure 4.16:** Oxygen addition (left) and temperature profile (right) at 150 psig.

The oxygen addition data shows negative consumption region for all heating rates in the 150 psig experiments at late times. We attribute this difference to oxygen addition onto coke surface. Using the oxygen addition data along with recorded temperature, the isoconversional fingerprint in Figure 4.17 was obtained.

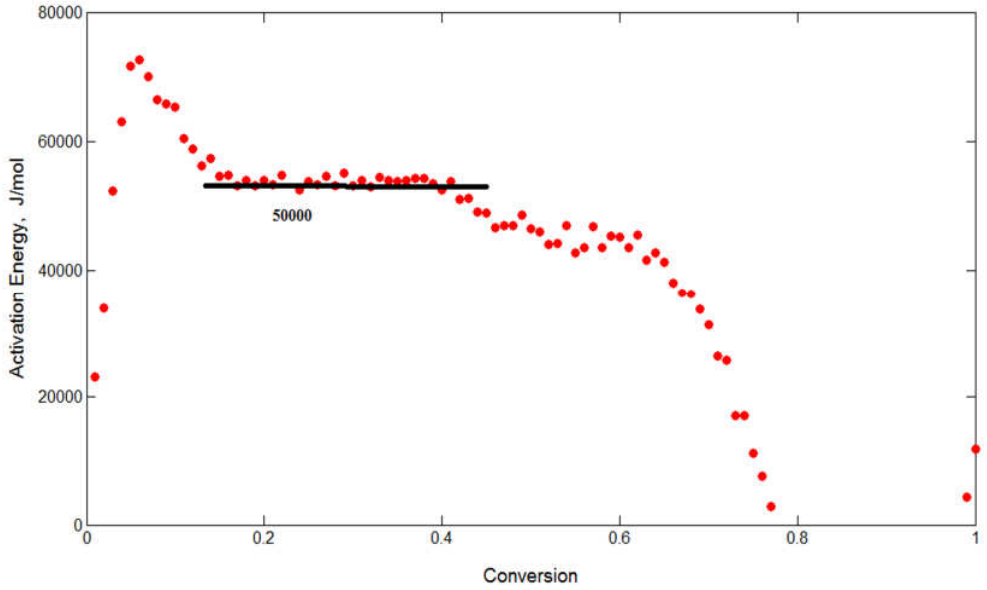


**Figure 4.17:** Isoconversional fingerprint for oxygen addition at 150 psig.

The LTO activation energy is estimated to be 50000 J/mol from Figure 4.17.

#### 4.3.2.3 Experiments at 200 psig

The RTO experiments were repeated at 200 psig to obtain isoconversional fingerprints and activation energies. Figure 4.18 shows the oxgyen and recorded temperature data at various heating rates.

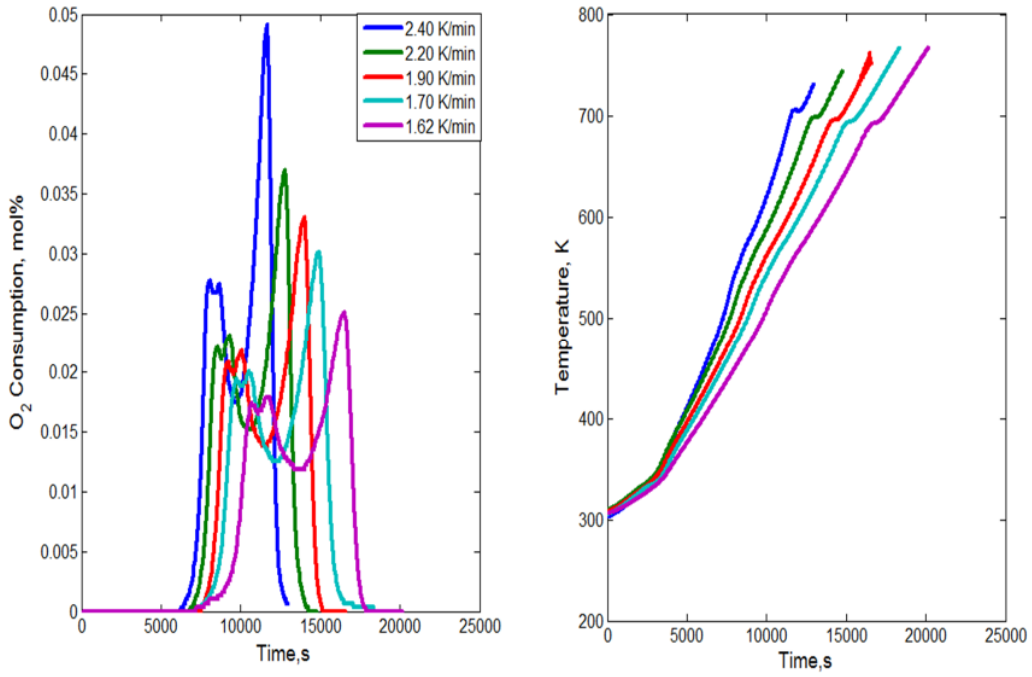


**Figure 4.18:** Oxygen consumption (left) and temperature profile (right) at 200 psig.

The oxygen data show a good consistency and an observation is made that higher heating rate oxygen consumption peak is higher.

The temperature data, however, does not change since the same heating rates were used and as seen clearly, the same minor errors observed in 100 and 150 psig experiments are also observed in 200 psig experiments. Using the oxygen data along with recorded temperature, the isoconversional method is applied to obtain the fingerprint in Figure 4.19.

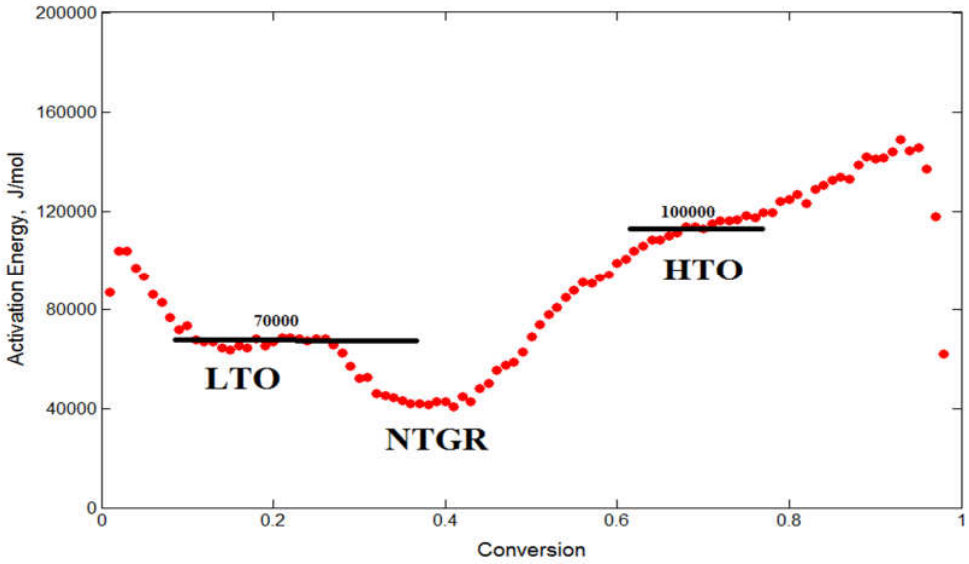


**Figure 4.19:** Isoconversional fingerprint for oxygen at 200 psig.

HTO activation energy value of 100000 J/mol was estimated from Figure 4.19. This activation energy value is higher than the previous estimated activation energies from the oxygen conversion fingerprint for the 100 and 150 psig experiments. An increasing trend of activation energy with pressure increase is observed. The produced carbon oxides are also graphed in Figure 4.20 and are also used in the isoconversional analysis to generate fingerprints as previously done in the other two pressure experiments.

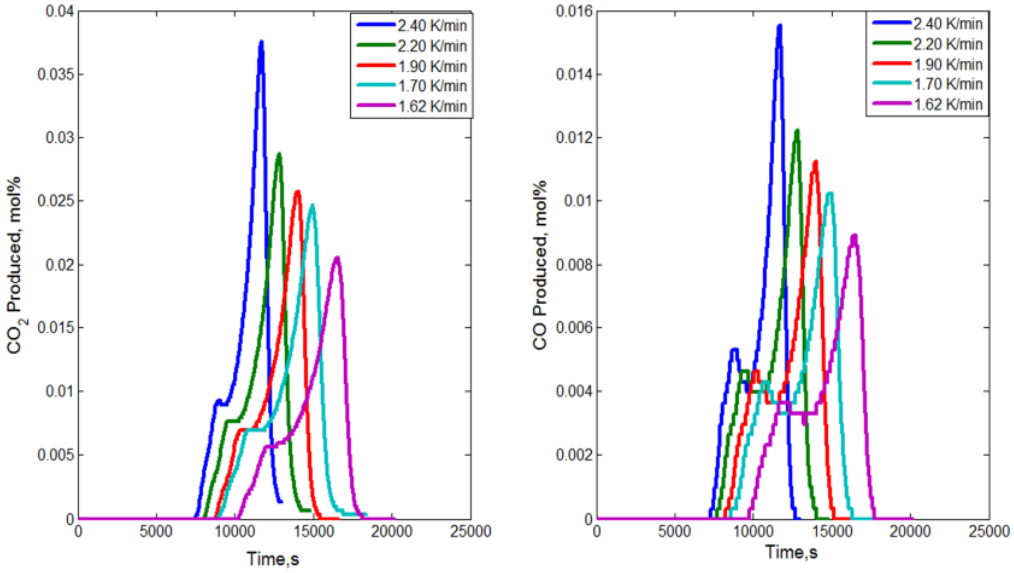


**Figure 4.20:** Produced carbon dioxide (left) and carbon monoxide (right) at 200 psig.

Carbon oxides data in Figure 4.20 show carbon dioxides production are more than monoxides as observed from previous experimental data. Using these data along with the recorded temperature of Figure 4.18, the isoconversional method is applied and fingerprints obtained. In Figure 4.21, a combined isoconversional fingerprints of oxygen, carbon dioxide and carbon monoxide are shown.

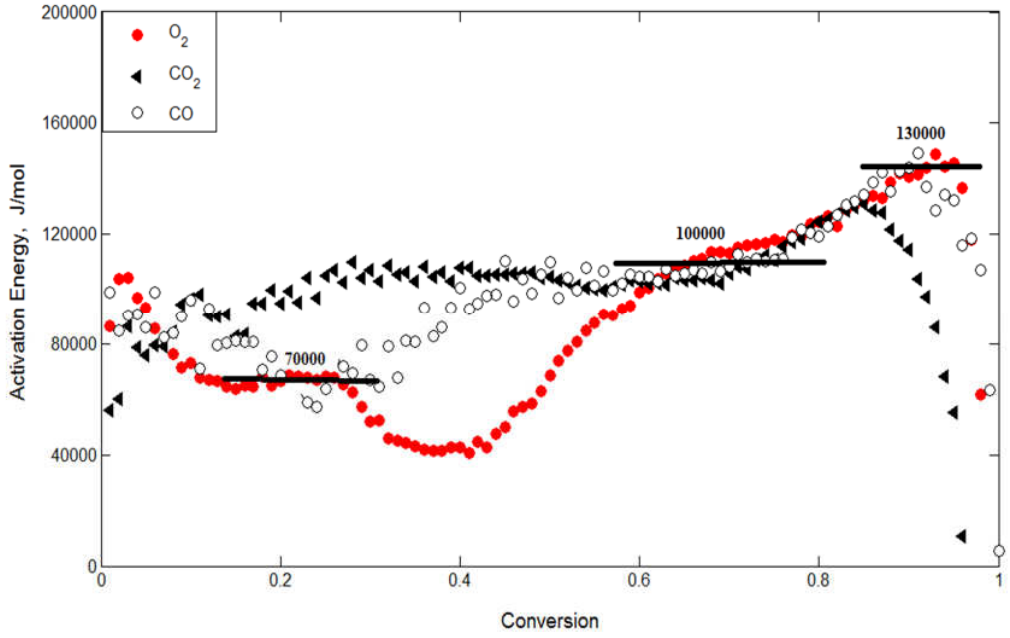


**Figure 4.21:** Combined isoconversional fingerprints for oxygen and carbon oxides at 200 psig.

The trends observed from Figure 4.21 are consistent with those of previous experiments. Figure 4.21 indicates three dominant reactions having activation energy values of 70000, 100000, and 130000 J/mol. NTGR for the produced carbon oxides fingerprints are shifted to the left of the NTGR of oxygen fingerprint.

This phenomenom has already been discussed in the 100 and 150 psig sections and the same reason is attributed to the 200 psig experiments. Using the amounts of oxygen not used in the production of carbon oxides is estimated at each heating rate and graphed along with recorded temperature data in Figure 4.22.

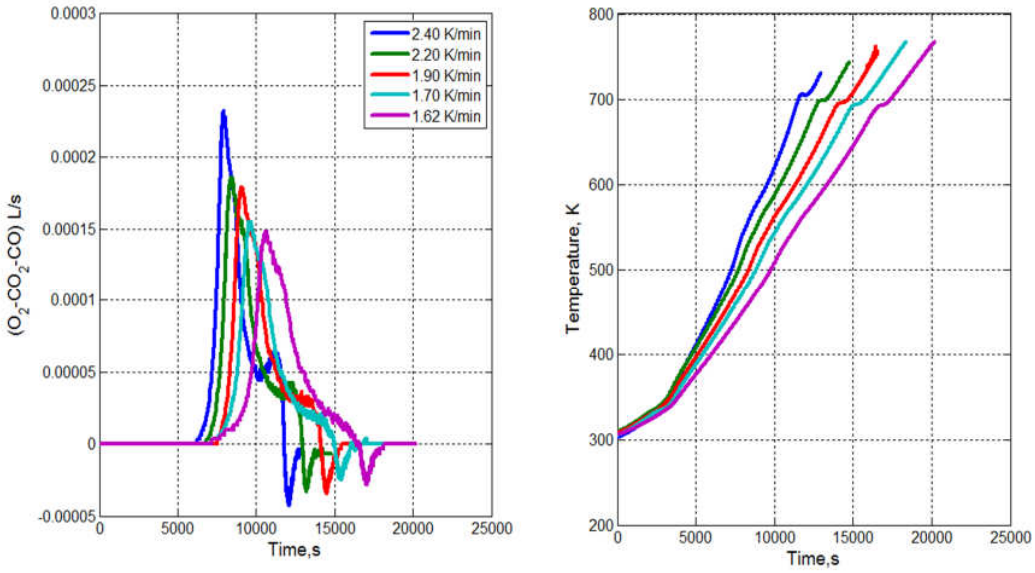


**Figure 4.22:** Oxygen addition (left) and temperature profile (right) at 200 psig.

The oxygen additon data shows a negative consumption region for all heating rates in late times. Again possible explanation may be that, in the initial stages of oxygen addition, some amounts of oxygen are stored in carbon oxygen bonds and this may lead to extra oxygen within the system. Using the oxygen addition data along with recorded temperature, the isoconversional fingerprint in Figure 4.23 was obtained.

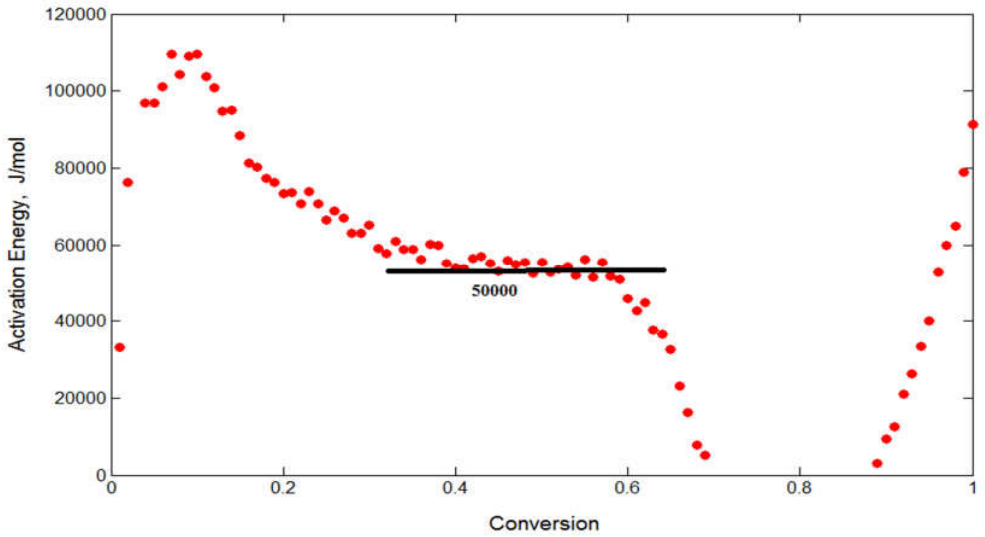


**Figure 4.23:** Isoconversional fingerprint obtained for oxygen addition at 200 psig. An LTO activation energy of 50000 J/mol is obtained.

#### 4.3.2.4 Experiments at 250 psig

Finally, the RTO experiments were repeated at 250 psig to observe any changes in the isoconversional fingerprints and activation energy values. The oxygen data along with recorded temperature are graphed in Figure 4.24.

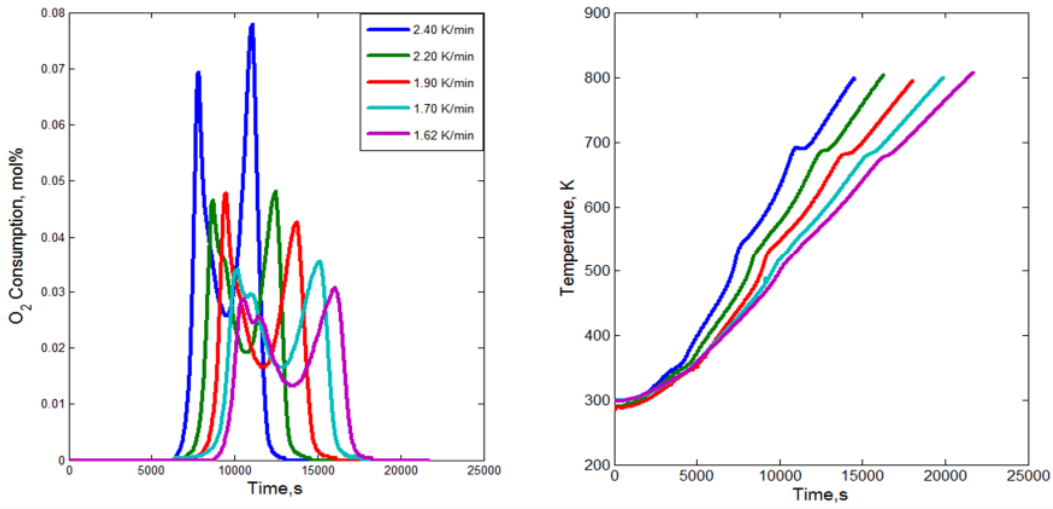


**Figure 4.24:** Oxygen consumption (left) and temperature profile (right) for 250 psig.

The temperature data and the oxygen consumed show a good consistency in Figure 4.24. Using the oxygen data and their temperature profiles, the isoconverisonal process was applied and the fingerprint in Figure 4.25 was obtained.

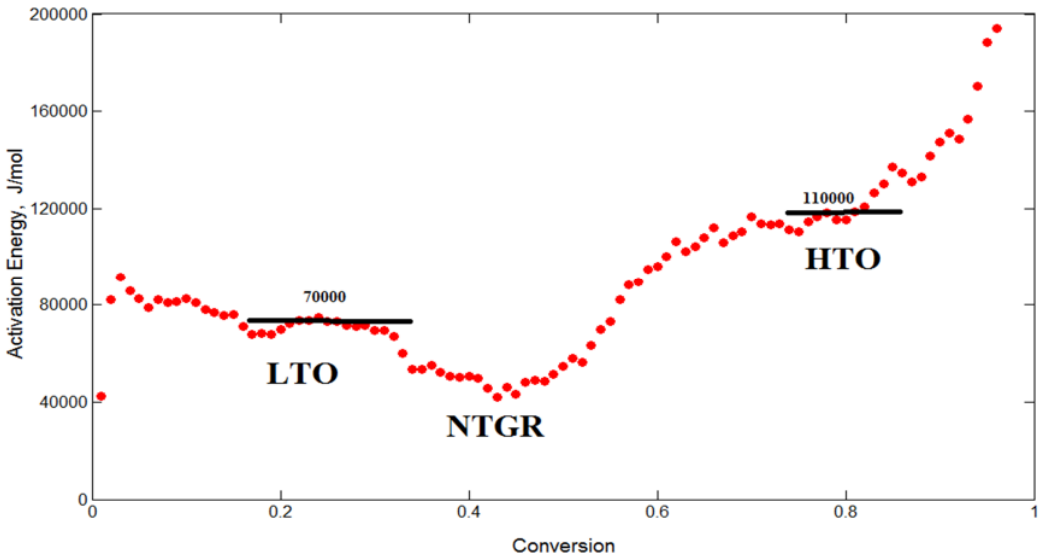


**Figure 4.25:** Isoconversional fingerprint for oxygen at 250 psig.

HTO activation energy value of 110000 J/mol was estimated from Figure 4.25. This activation energy value is higher than the previous estimated activation energy from the oxygen conversion fingerprint for 100, 150 and 200 psig. This suggests an increase in activation energy with corresponding increase in pressure.

The produced carbon oxides are also graphed in Figure 4.26 and are also used in the isoconversional analysis to obtain fingerprints as previously done in the other three experiments.

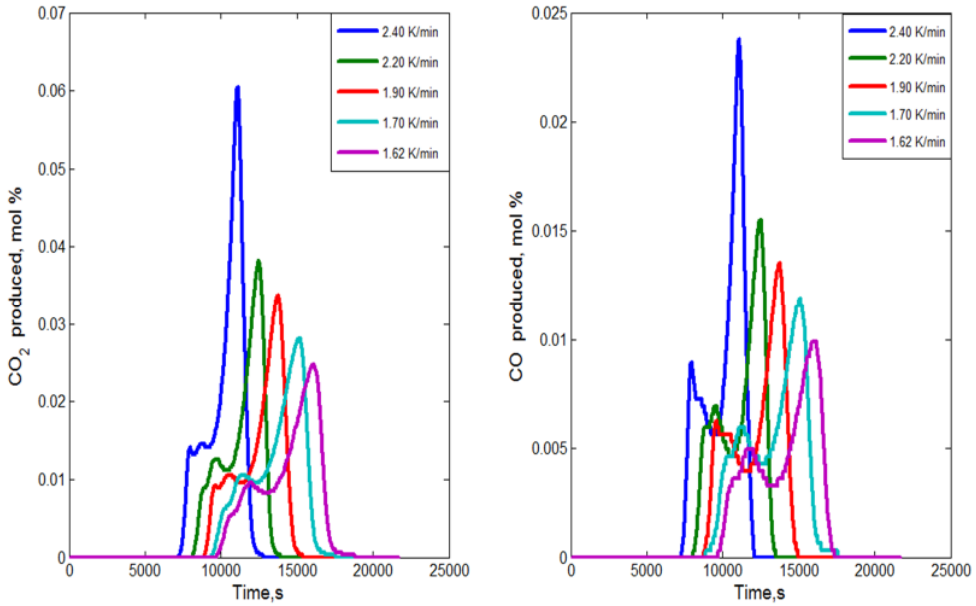


**Figure 4.26:** Produced carbon dioxide (left) and carbon monoxide (right) at 250 psig.

From the carbon oxides data in Figure 4.26, the amounts of carbon dioxide are more than that of monoxides as seen from previous experimental data.

Using these data along with the recorded temperature of Figure 4.24, the isoconversional method is applied and fingerprints obtained. In Figure 4.27, a combined isoconversional fingerprints of oxygen, carbon dioxide, and carbon monoxide are shown.

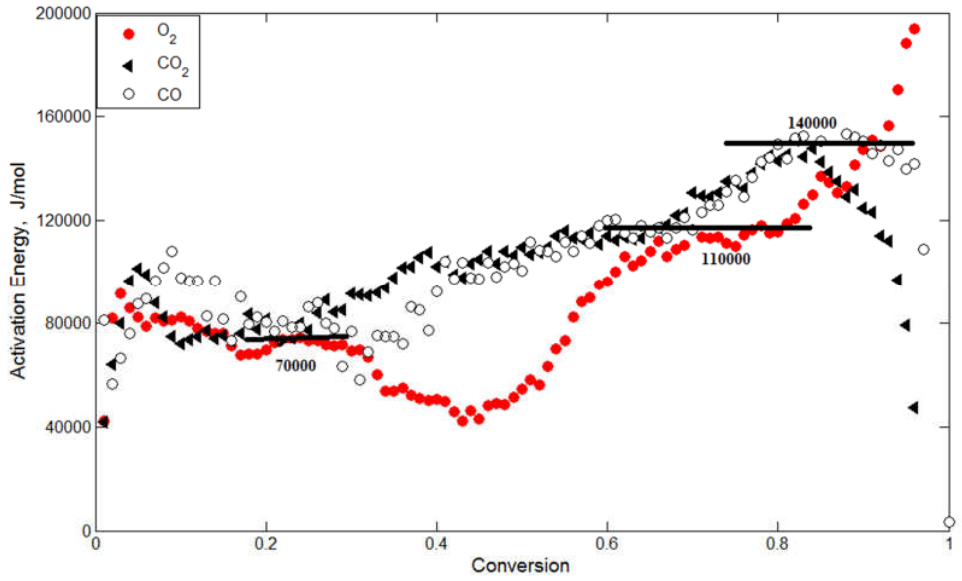


**Figure 4.27:** Combined isoconversional fingerprints for oxygen and carbon oxides at 250 psig

Fingerprints obtained for the carbon oxides do not fit the NTGR of oxygen but it is an expected behaviour since in the LTO region some consumed oxygen is used to form water and other unknown reactions. Again a mole balance is employed on the oxygen and carbon oxides data to find the molar amounts of oxygen used for oxygen addition reactions. We obtain the raw data in Figure 4.28.

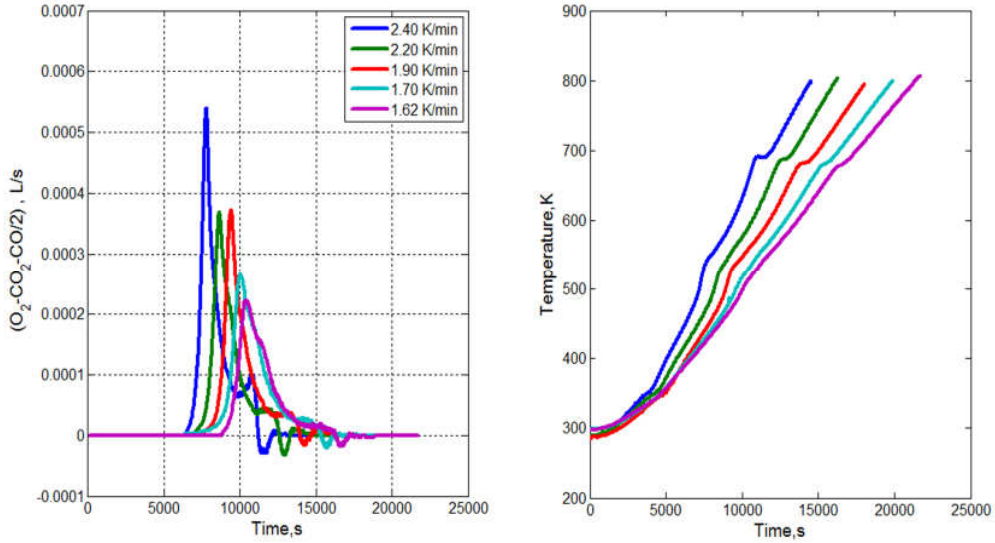


**Figure 4.28:** Oxygen addition (left) and temperature profile (right) at 250 psig.

We observe negative consumption in the oxygen data as previously seen from the other experiments. Using the raw data for remaining oxygen and recorded temperature values, we used the isoconversional technique to generate the fingerprint in Figure 4.29.

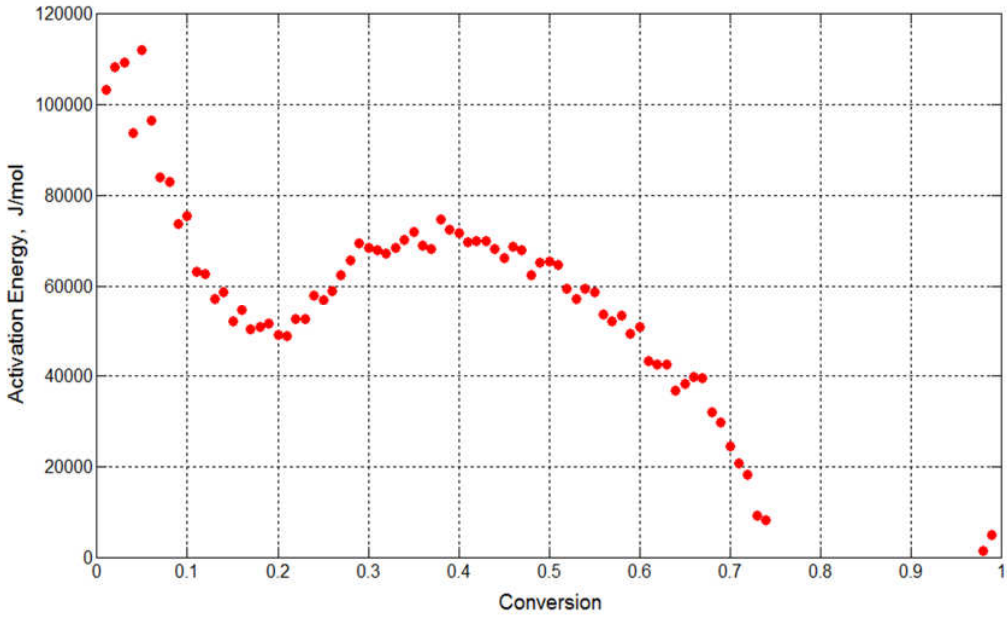


**Figure 4.29:** Isoconversional fingerprint obtained for oxygen addition at 250 psig.

In this case, we were unable to estimate an activation energy for the LTO reaction. We attribute this issue to experimental error. We suspect one of the experiments is inconsistent.

Çınar (2011) explains that, inconsistent reactions may result from allowing sample to wait in a reactive environment for a few hours without beginning experiment. This may lead to changes in the oxygen consumption and heat released.

Secondly, if packing of the sample differs from other sets of experiments, the oxygen consumption curves may show different trends. Any other unforseen mistakes in the sample preparation or experimental setup may also lead to inconsistent results.

### 4.4 Comparison of Isoconversional Results at Different Pressures

Figure 4.30 shows the oxygen consumption, carbon oxides production and temperature profiles obtained at 1.62 K/mim heating rate for all operating pressures. A good consistency is established in oxygen consumption, carbon oxides production and programmed temperature profiles. It seems the estimated consumption and production values are quite close.

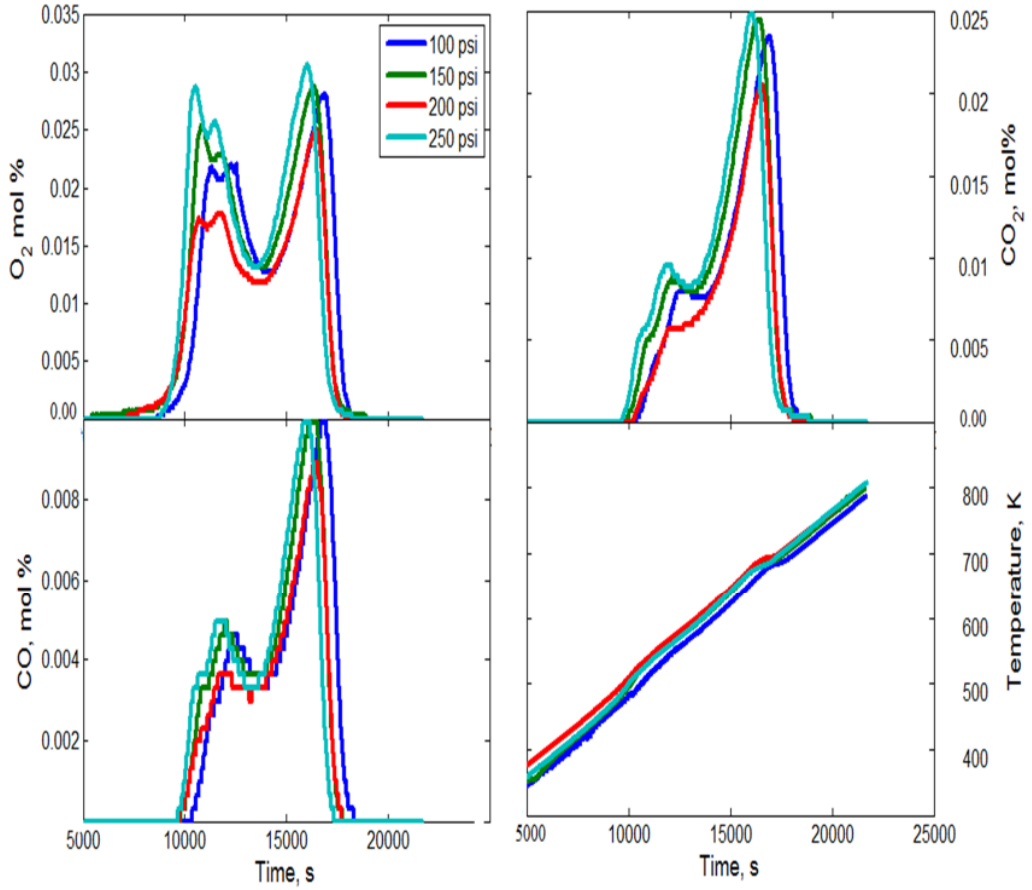


**Figure 4.30:** Oxygen consumption, carbon oxides production and temperature profiles at 1.62 K/min for various pressures.

Here, we compare all oxygen fingerprints obtained at the various pressures of 100, 150, 200, and 250 psig to observe pressure effect on activation energy values. Figure 4.31 shows the isoconversional fingerprints for consumed oxygen obtained at various operating pressures used in this study.

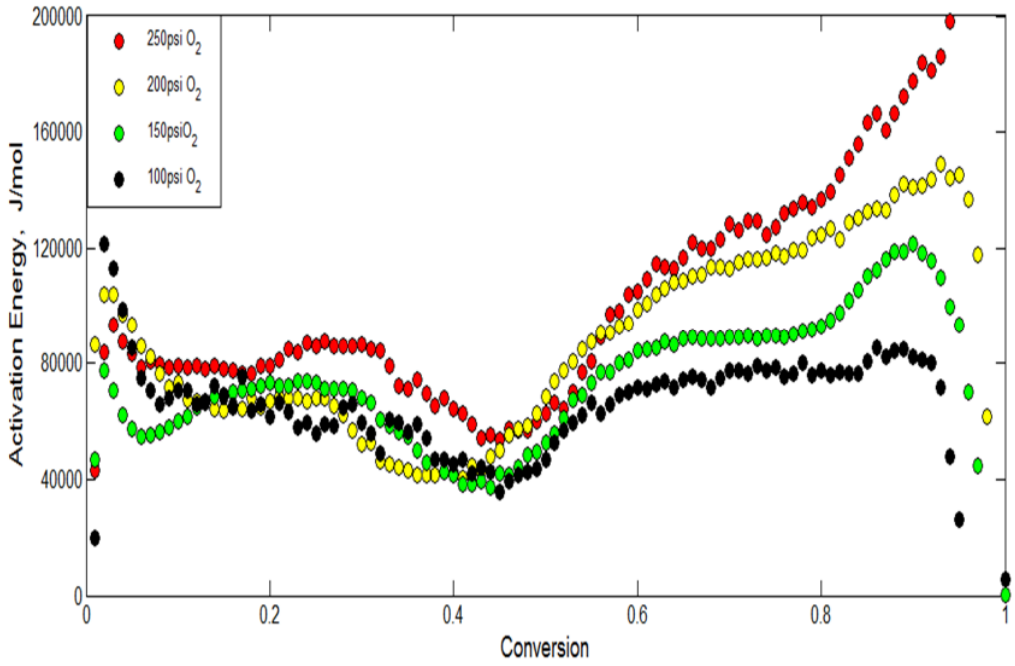


**Figure 4.31:** Oxygen fingerprint comparisons at 100, 150, 200, and 250 psig.

Figure 4.31 gives a clear trend that for the HTO of Bati Raman crude oil, effective activation energy increases with increasing pressure.

Table 4.2 shows the estimated activation energy values obtained in the HTO regions using the isoconversional fingerprint diagrams of Figure 4.31.

**Table 4.2:** HTO activation energies evaluated with the isoconversional method.

| Pressure Psi | HTO J/mol |
|---|---|
| 100 | 70000 |
| 150 | 82000 |
| 200 | 100000 |
| 250 | 110000 |

### 4.5 Comparison of Fassihi and Isoconversional Results.

Average activation energy for various heating rates at a particular pressure were calculated in Table 4.1 for Fassihi's method in the HTO regions and compared with activation energies evaluated with the isoconversional method in Table 4.3.

**Table 4.3:** Comparison of HTO activation energies evaluated with Fassihi and Isoconverional methods

| Pressure psig | Fassihi (Averaged) J/mol | Isoconversional Analysis J/mol | Deviation (%) |
|---|---|---|---|
| 100 | 85000 | 70000 | 21.4 |
| 150 | 108000 | 82000 | 31.7 |
| 200 | 115000 | 100000 | 15.0 |
| 250 | 140000 | 110000 | 27.3 |

$$Deviation = \frac{Fassihi's \quad Method - Isoconversional \quad Method}{Isoconversional \quad Method} \tag{4.32}$$

Therefore at 150 psig,

$$Deviation = \frac{108000 - 82000}{82000} = 0.317(31.7\%) \tag{4.33}$$

We have intentionally used the word deviation instead of error to avoid any controversies.

We used Equation 4.32 in the calculation of deviation of activation energies estimated with Fassihi's method and the isoconversional method. By the use of Equation 4.32, column (4) of Table 4.3 was obtained. Equation 4.32, illustrates the calculation procedure at a pressure of 150 psig for which a deviation of 0.317 (31.7 %) was obtained. Average deviation as shown in Table 4.3 was calculated from the total sum of the deviations and divided by four to give 24 %.

### 4.6 Reaction Models at Various Pressures

Reaction models for Bati Raman crude oil are proposed at all operating pressures. Using molecular weight of oil (500 g/gmol), H/C ratios, LTO and HTO ratios of $CO_2/CO$ and $O_2/CO_2$; the atomic mole ratios and molar mass of coke are calculated based on the reaction model proposed by Çınar (2011) which is based exclusively on the various reaction regions shown on the isoconversional fingerprint. The model is described by Equation 4.34:

$$\begin{aligned}
&\text{Reaction } 1: && Oil + s_{1,1}O_2 \xrightarrow{k_1} s_{1,2}Coke_1 + s_{1,3}H_2O + s_{1,4}CH_4 \\
&\text{Reaction } 2: && Coke_1 + s_{2,1}O_2 \xrightarrow{k_2} s_{2,2}CO_2 + s_{2,3}CO + s_{2,4}H_2O \\
&\text{Reaction } 3: && Coke_1 \xrightarrow{k_3} s_{3,1}Coke_2 \\
&\text{Reaction } 4: && Coke_2 + s_{4,1}O_2 \xrightarrow{k_4} s_{4,2}CO_2 + s_{4,3}CO + s_{4,4}H_2O
\end{aligned} \qquad \textbf{(4.34)}$$

$S_{i,j}$ represents the stoichiometric coefficients. The first reaction is termed as the oxygen addition reaction. The reaction between oil and oxygen produces coke, water and little amounts of methane which is usually neglected during the balancing of the molar atoms in reaction. Reaction one occurs in the LTO region. The second reaction also occurs in the LTO region and leads to production of carbon oxides and water as its products. The third reaction occurs in the negative temperature region where the oxygen consumption reduces even as temperature increases. The reduction in oxygen consumption may be attributed to the usage of the first coke formed in the LTO region which eventually gets deposited on the rock matrix but ends with a reduced molecular weight as coke2. Finally, in the HTO region reaction four occurs as the oxygen reacts with the second coke deposited on the rock matrix. The products formed are carbon oxides and water. The various proposed reaction models at different operating pressures are summarized with Equations 4.37-4.40. H/C ratios, $CO_2/CO$ and $O_2/CO$ ratios used in the reaction model formulations are also discussed in subsequent sections.

### 4.6.1 H/C ratios

H/C ratios are estimated from the molar amounts of consumed and produced gases. H/C ratios are required in estimating the air requirements and also in obtaining molar ratios in the oxidation reaction of the crude oil. Here we assume that all the oxygen molecules that do not form carbon oxides form water. The number of hydrogen (H) and carbon (C) are estimated from Equations 4.35 and 4.36 respectively.

$$H = 4 \times \left(\frac{\sum O_2 - CO_2 - CO/2}{22.4}\right) \quad \textbf{(4.35)}$$

Here, $O_2$ is total oxygen consumption in standard liters, $CO_2$ and $CO$ are total carbon dioxide and carbon monoxide production in standard liters.

$$C = \frac{\sum (CO_2 + CO)}{22.4} \quad \textbf{(4.36)}$$

Applying Equations 4.35 and 4.36, the estimated H/C values are recorded in Table 4.4.

**Table 4.4:** H/C ratios estimated at various pressures.

| Pressure Psi | 2.40 K/min | 2.20 K/min | 1.90 K/min | 1.70 K/min | 1.62 K/min | Average |
|---|---|---|---|---|---|---|
| 100 | - | 1.85 | 1.74 | 1.71 | 1.49 | 1.70 |
| 150 | 1.64 | 1.51 | 1.78 | 1.55 | 1.52 | 1.60 |
| 200 | 1.77 | 1.71 | 1.74 | 1.50 | 1.81 | 1.71 |
| 250 | 1.53 | 1.84 | 1.64 | 1.85 | 1.67 | 1.70 |

### 4.6.2 CO2/CO and $O_2$/CO ratios

These ratios were obtained from the plot of time intervals for LTO and HTO regions vs $CO_2$/CO and $O_2$/CO ratios using the 1.62 K/min heating rate for each operating pressure used. The 1.62 K/min expirements were chosen because they usually span a much greater time. It must be mentioned that, for $O_2$/CO ratio we use $O_2 = CO_2 + CO/2$ in the ratio calculation. Plots of $CO_2$/CO, $O_2$/CO vs time in HTO region are shown on Figure 4.32. From the plot, the straight line portion is chosen as the ratio for each of them. Using this method, $CO_2$/CO is 2.4 and $O_2$/CO is recorded as 1.2 for 1.62 K/min (100 psig). Table 4.5 summarizes the ratios obtained at the different operating pressures.

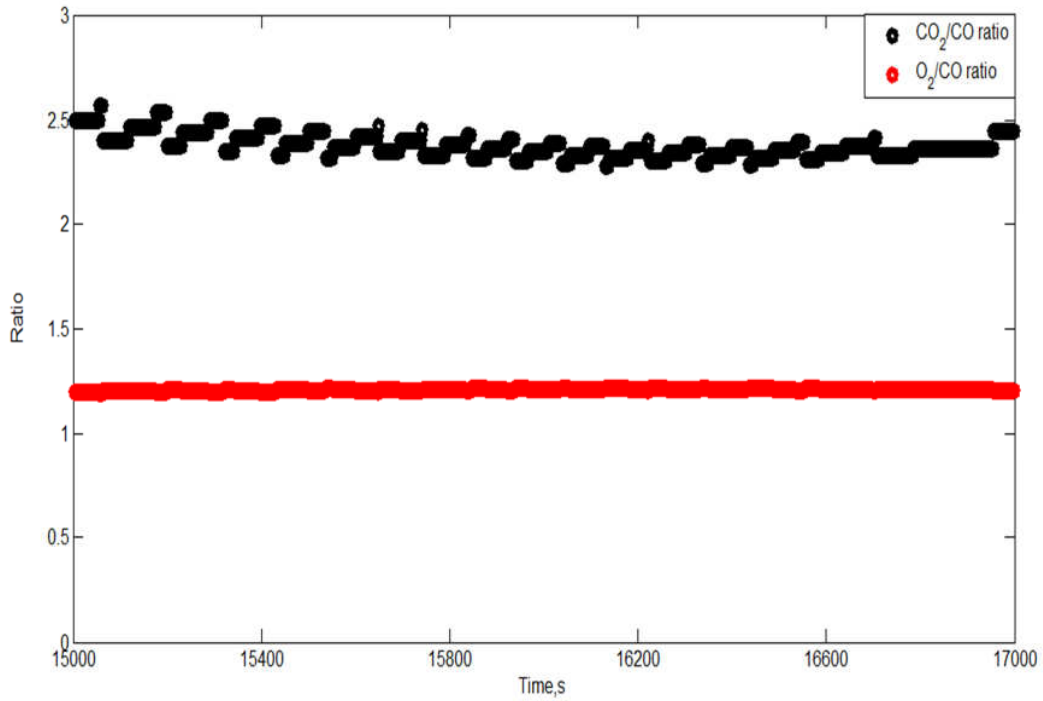


**Figure 4.32:** $CO_2/CO$ and $O_2/CO_2$ ratios vs Time for 1.62 K/min (100 psig).

**Table 4.5:** $CO_2/CO$ and $O_2/CO_2$ ratios estimated at various pressures.

| Pressure Psi | LTO $CO_2/CO$ | LTO $O_2/CO_2$ | HTO $CO_2/CO$ | HTO $O_2/CO_2$ |
|---|---|---|---|---|
| 100 | 1.50 | 1.33 | 2.40 | 1.20 |
| 150 | 1.61 | 1.30 | 2.40 | 1.21 |
| 200 | 1.55 | 1.32 | 2.30 | 1.22 |
| 250 | 1.66 | 1.32 | 2.42 | 1.21 |

### 4.6.3 Reaction models proposed

Formulation of stoichiometric reactions 1 to 4 for Equation 4.38 are briefly explained using isoconversional results obtained for 150 psig experiments given in section 4.3.2.2. Stoichiometric coefficients for the Reaction 4 is obtained from the average $O_2$ / CO and $O_2$ / $CO_2$ ratios in the HTO region. The same ratios, this time in the LTO region, are used for the stoichiometry of the Reaction 2.

Using the molar mass of oil (500 g/gmol), H/C ratio, and mole balances for oxygen, water and $coke_1$, stoichiometry for the Reaction 1 is obtained. Finally, the ratio of molecular weights of $coke_1$ to $coke_2$ is used to formulate the Reaction 3.

Evaluation of activation energies $E_1$ to $E_4$ are also explained briefly using 150 psig data. For the Reaction 1 (oxygen addition reactions), $E_1$ (50000 J/mol) is obtained from Figure 4.17 for the oxygen addition reactions occurring in the LTO region (0.2-0.4) where a stabilized region is observed. $E_2$ (70000 J/mol) was obtained from Figure 4.15 in the stabilized LTO region (0.1 - 0.3) where carbon oxides production are dominant. $E_3$ (110000 J/mol), which generally develops much later due to a possible shift in a dominant reaction with increasing temperature, was obtained in HTO region (0.8 - 1) from Figure 4.15. Finally, $E_4$ (80000 J/mol) was obtained from Figure 4.15 in the HTO region (0.6 – 0.8) where a stabilized region is observed. These steps were followed for all reactions at all operating pressures.

**Reaction model – 100 psig**

$$\text{Reaction 1: } Oil + 18.94O_2 \xrightarrow{k_1} 17.40Coke_1 + 26.98H_2O \quad E_1 = 50000 \ J/mol$$

$$\text{Reaction 2: } Coke_1 + 2O_2 \xrightarrow{k_2} 1.5CO_2 + CO \qquad E_2 = 60000 \ J/mol$$

$$\text{Reaction 3: } Coke_1 \xrightarrow{k_3} 1.79Coke_2 \qquad E_3 = 70000 \ J/mol \qquad \textbf{(4.37)}$$

$$\text{Reaction 4: } Coke_2 + 1.2O_2 \xrightarrow{k_4} CO_2 + 0.4CO \qquad E_4 = 70000 \ J/mol$$

$$MW_{coke_1} = 30 g/gmol; \qquad MW_{coke_2} = 16.8 g/gmol$$

Note that activation energy for reaction three could not be observed for 100 psig. In this case reaction three is much faster than reaction four and the two reactions are probably controlled by the same mechanism and therefore same HTO activation energy of 70000 J/mol is estimated for both reactions.

**Reaction model – 150 psig**

$$\begin{aligned}
&\text{Reaction 1:}\quad Oil + 17.53O_2 \xrightarrow{k_1} 16.85Coke_1 + 35.06H_2O \quad E_1 = 50000 \ J/mol \\
&\text{Reaction 2:}\quad Coke_1 + 2.1O_2 \xrightarrow{k_2} 1.6CO_2 + CO \qquad\qquad E_2 = 70000 \ J/mol \\
&\text{Reaction 3:}\quad Coke_1 \xrightarrow{k_3} 1.83Coke_2 \qquad\qquad E_3 = 110000 \ J/mol \\
&\text{Reaction 4:}\quad Coke_2 + 1.21O_2 \xrightarrow{k_4} CO_2 + 0.42CO \qquad E_4 = 82000 \ J/mol \\
&\qquad MW_{coke_1} = 31 g/gmol; \qquad MW_{coke_2} = 17.04 g/gmol
\end{aligned} \tag{4.38}$$

**Reaction model – 200 psig**

$$\begin{aligned}
&\text{Reaction 1:}\quad Oil + 18.49O_2 \xrightarrow{k_1} 17.06Coke_1 + 36.98H_2O \quad E_1 = 50000 \ J/mol \\
&\text{Reaction 2:}\quad Coke_1 + 2.05O_2 \xrightarrow{k_2} 1.55CO_2 + CO \qquad E_2 = 70000 \ J/mol \\
&\text{Reaction 3:}\quad Coke_1 \xrightarrow{k_3} 1.77Coke_2 \qquad\qquad E_3 = 130000 \ J/mol \\
&\text{Reaction 4:}\quad Coke_2 + 1.22O_2 \xrightarrow{k_4} CO_2 + 0.44CO \qquad E_4 = 100000 \ J/mol \\
&\qquad MW_{coke_1} = 30.06 g/gmol; \qquad MW_{coke_2} = 17.28 g/gmol
\end{aligned} \tag{4.39}$$

**Reaction model – 250 psig**

$$\text{Reaction 1:}\quad Oil + 17.53O_2 \xrightarrow{k_1} 16.85Coke_1 + 35.06H_2O \quad E_1 = 50000\ J/mol$$

$$\text{Reaction 2:}\quad Coke_1 + 2.1O_2 \xrightarrow{k_2} 1.6CO_2 + CO \qquad E_2 = 70000\ J/mol$$

$$\text{Reaction 3:}\quad Coke_1 \xrightarrow{k_3} 1.83Coke_2 \qquad E_3 = 110000\ J/mol \qquad \textbf{(4.40)}$$

$$\text{Reaction 4:}\quad Coke_2 + 1.21O_2 \xrightarrow{k_4} CO_2 + 0.42CO \qquad E_4 = 82000\ J/mol$$

$$MW_{coke_1} = 31 g/gmol; \qquad MW_{coke_2} = 17.04 g/gmol$$

## 5. CONCLUSIONS AND FUTURE RESEARCH

The RTO experiments were conducted with Bati Raman crude (12$^{o}$ API) and gas composition curves obtained from plotting gas concentration versus time at each heating rate at different pressures all showed three different reaction regions (LTO, MTR and HTO) as observed by Fassihi (1981), Fassihi et al. (1984b), Bağci (2005), Moore et al. (1997), Çınar (2011), and several other investigators in their kinetics studies. Conventional model by Fassihi (1981) and the isoconversional method were applied to estimate activation energy for Bati Raman crude. The experimental results indicate that during LTO, not all consumed oxygen is used for the formation of carbon oxides but rather other competing reactions occur which makes use of the consumed oxygen. The isoconversional fingerprints for such competing reactions in the LTO region were generated.

Comparison of oxygen consumption at various heating rates indicates that peak oxygen consumption increases with increasing heating rate. Isoconversional fingerprints obtained using consumed oxygen at the various pressures confirm that estimated values of activation energy increase with pressure increase. From Table 4.1, at a particular fixed pressure, activation energies decrease with increasing heating rate and a trend of activation energy increase with pressure is observed for Fassihi's method. Bağci et al. (1987), Bağci (2005) conducted kinetic studies on Bati Raman crude with crushed limestones and observed an increase of activation energy with pressure in the HTO region using Fassihi's method. For the five heating rates, Fassihi's method gives five different activation energy values whereas the isoconversional method gives only one activation energy value. An increasing trend of activation energy with pressure increase is observed for both methods as shown by Table 4.3. Another observation is that, average effective activation energies estimated with Fassihi's method are higher than those obtained with the isoconversional method. Average activation energy deviation of 24 percent is calculated between both methods. Although the average activation energy deviation

between both methods does not seem too much in this study, the isoconversional method has the advantage of distinguishing different regions of reactions in its fingerprint as seen from the results of the various fingerprints generated at the various operating pressures. Perhaps the only disadvantage of the isoconversional method is the series of kinetics runs (five) that needs to be conducted. This disadvantage does not represent a gain for the Fassihi's method because, Semenov (1935) and Kovscek et al. (2013) asserts that, a single reaction or characterization is insufficient to fully probe the complex and numerous series (parallel) reactions, as well as the highly exothermic reactive transport, that are characteristic of ISC.

Reaction models were proposed for Bati Raman crude oil oxidation at various operating pressures. The reactions at various pressures shows a good consistency from the estimation of reaction species ratios. Average H/C ratio of 1.7 was estimated for all experiments at various pressures from Table 4.4. Average $CO_2$/CO ratio was estimated as 1.6 from Table 4.5. Average molecular weights for $Coke_1$ and $Coke_2$ were estimated as 30.88 g/gmol and 17.04 g/gmol respectively The almost identical values for these ratios at all operating pressures may be attributed to the sandstone matrix used in the experiment. We believe the sandstone matrix does not not take part in the oxidation reactions and hence the low values. Bağci et al. (1987), in their comparative study of matrix effect with Bati Raman crude concluded that, sandstone matrix produces less (twice lower) the amounts of CO2/CO and H/C ratio in limestone matrix for a 17.8$^o$ API oil. Perhaps, the close proximity of the stoichiometry of the reactions at various pressures indicate a good trend of consistent reaction schemes.

Finally, using the isoconversional fingerprint of activation energy vs conversion, the Bati Raman crude oil is predicted as a good canditate for combustion in a sandstone matrix as the generated fingerprints does not exhibit any energy barriers in their negative temperature regions (NTGR). Sandstone matrix is used in this study for reasons such as: owing to the very large permeability of our sandstone, we eliminate the effects of oxygen diffusion and target the reaction kinetics of the Bati Raman oil itself. Within the literature, it is reported that crude oil oxidation in limestone environment is complex and therefore for academic purposes and as a start, we believe there is a justification to use sandstone matrix eventhough Bati Raman Field lithology is mostly composed of limestone rock matrix.

Future research work will concentrate on the kinetic study of Bati Raman crude in limestone matrix to observe the reactions and pressure effect on activation energy values in comparison with the homogenous sandstone matrix used as well as with varying particle size. Matching of kinetic experimental results to simulated data and upscaling of laboratory results to field scale will be looked at.

## REFERENCES


**Adegbesan, K.O.** (1982). Kinetics study of low temperature oxidation of Athabasca bitumen, PhD Thesis. Calgary University, Alberta, Canada.

**Alexander, J.D., Martin, W.L., and Dew, J.N.** (1962). Factors affecting fuel availability and composition during in-situ combustion. *Journal of Petroleum Technology:* 14(10), 1154 – 1164.

**Babu, D.R and Cormack, D.E.** (1984). Effect of low temperature oxidation on the composition of Athabasca bitumen. *Fuel*, 63 (6) : 858 – 861.

**Bae, J.H** (1977). Characterization of crude oil for fireflooding using thermal analysis methods. *SPE Journal*, 17(3): 211 – 218.

**Bağci, S.** (2005). Effect of pressure on combustion kinetics of heavy oils.

*Energy sources,* 27(9): 887 – 898.

**Bağci, A.S, Kök, M.V., and Okandan, E.** (1987). Combustion reaction kinetics in limestones containing heavy oils.

SPE conference paper – 15737 – MS. Middle East oil show, Bahrain.

**Bardon, C and Gadelle, C.O.** (1977). Essai de laboratoire pour l'etude de la combustion in situ. Paper presented at the 1977 French Soviet symposium on enhanced oil recovery, Moscow.

**Benham, A.L., and Poettmann, F.H.** (1958). Thermal recovery process – An analysis of laboratory combustion data. *Trans. AIME.* 213, 406 – 408.

**Belgrave, J.D.M., Moore, R.G., Ursenbach, M.G and Bennion, D.W.** (1993).

A comprehensive approach to in situ combustion modeling.

*SPE Advanced Technology*, 1(1): 98 – 107.

**Berry, H.J.** (1968). An experimental investigation of forward and combustion oil recovery. PhD Thesis. Texas A and M University, College Station.

**Bousaid, I.S and Ramey, H.J.Jr.,** (1968). Oxidation of crude oil in porous media. *SPE Journal*, 8(2):137 – 148.

**Brigham, W.E and Castanier, L.** (2003). In situ combustion handbook. SPE, 2003.

**Burger, J.G and Suhuquet, B.C.** (1972). Chemical aspects of the in situ combustion – Heat of combustion and kinetics.

*SPE Journal*, 12(5): 410 – 422.

**Burger, J.G.** (1976). Spontaneous ignition in oil reservoirs.

*SPE Journal*, April: 73 – 81.

**Cady, G.V and Satchwell, R.M.** (1985). Process variables of enriched air combustion: An experimental study. SPE paper 14525 presented at the SPE Eastern regional meeting, Morgantown, West Virginia (USA).

**Carberry, J.J.** (1976). Chemical and catalytic reaction engineering.

McGraw-Hill Book Company. New York. USA.

**Castanier, L.M., and Brigham, W.E.** (2003). Upgrading of crude oil via in situ combustion.

*Journal of Petroleum Science and Engineering*, 39(1–2): 125 – 136.

**Çınar, M., Castanier, L.M., and Kovscek, A.R.** (2011). Predictability of crude oil in situ combustion by the isoconversional Kinetic Approach. *SPE Journal*, 16(3): 537 – 547.

**Çınar, M.** (2011). Kinetics of crude oil combustion in porous media interpreted

using isoconversional analysis methods. PhD Thesis. Stanford

University, California. USA.

**Dabbous, M.K., and Fulton, P.F.** (1974). Low temperature oxidation reaction kinetics and effect on the in-situ combustion process.

*SPE Journal*, 14(3): 253 – 262.

**Dietz, D.N and Weijdema, J.** (1963). Wet and partially quenched combustion. *Journal of Petroleum Technology*, April: 411 – 415.

**Etebar, S.** (1995). Captain innovative development approach. SPE 30369.

In proceedings of SPE offshore Europe conference. Aberdeen, UK. September 5 – 8.

**Farouq Ali, S.M.** (1972). A current appraisal of in situ combustion field tests.

*Journal of Petroleum Technology*, 14(4): 477 – 86.

**Fassihi, M.R.** (1981). Analysis of fuel oxidation in in-situ combustion oil recovery. PhD thesis. Stanford University. California. USA.

**Fassihi, M.R., Brigham, W.E., and Ramey, H.J.** (1984a). Reaction kinetics of in

situ combustion. Part 2 –Modeling. *SPE Journal*, 24(4): 399 – 407.

**Fassihi, M.R., Brigham, W.E., and Ramey, H.J.** (1984b). Reaction kinetics of in

situ combustion. Part 2–Modeling. *SPE Journal*, September: 399 – 416.

**Freitag, N.P., and Verkoczy, B.** (2005). Low temperature oxidation of oils in terms of Sara fractions. Why Simple reaction models don't work.

*Journal of Canadian Petroleum Technology*, 44(3): 54 – 61.

**Friedman, H.L. (**1964**)**. Kinetics of thermal degradation of char-forming plastics from thermogravimetry. Application to phenolic plastic.

*Journal of Polymer Science*, Part C: Polymer symposia 6(1): 183–195.

**Gates, C.G and Ramey, H. J. Jr.** (1958). Field results of South Belridge thermal recovery experiment. *Trans, AIME*, Vol. 213, 236 – 244.

**Hayashitani, M.** (1978). Thermal cracking of Athabasca bitumen. PhD Thesis

The University of Calgary, Alberta, Canada.

**Howard, F.A.** (1923). Method of operating oil wells. USA Patent No. 1473348.

**Kovscek, A.R., Castanier, L.M., and Gerritsen, M.G.** (2013). Improved predictability of in situ combustion enhanced oil recovery.

*SPE Journal paper*, SPE 165577-PA. 16 (02): 172 – 182.

**Mamora, D.D.** (1993). Kinetics of in situ combustion. PhD Thesis.

Stanford University, California, USA.

**Meyerhoff, A.A and Meyer, R.F.** (1987). Exploration for heavy crude oil and natural bitumen in the USSR, Mongolia and China. AAPG studies in geology Tulsa, OK. 25: 31 – 101.

**Moore, R.G., Belgrave, J.D.M., and Ursenbach, M.G.** (1997). In situ combustion in heavy oil reservoirs – Problems and Perspectives. *In situ*: 21:1 – 26.

**Moss, J.T., White, P.D., and McNiel, J.S. Jr.** (1959). In situ combustion process results of a five well field experiment in Southern Oklahoma.

*Journal of Petroleum Technology*, April: 55-64; *Trans AIME*, 216.

**Ramey, H.J. Jr.** (1959). Transient heat conduction during radial movement of a cylindrical heat source – Application to the thermal recovery process. *Trans AIME*, 216, 115 – 122.

**Sarathi, P.S** (1998). In situ combustion handbook – Principles and practices.

Report DOE/PC/91008 - 0374, OSTI ID3175.

**Smith, J.M**. (1970). Chemical engineering kinetics. McGraw-Hill Book Company, New York.

**Tadema, H.J.** (1959). Mechanism of oil production by underground combustion. 5th World petroleum congress section II. Paper 22, 279 – 287.

**Tadema, H.J and Weijdema, J.** (1970). Spontaneous ignition of oil sands. *Oil and Gas Journal*, 68(50): 77 – 80.

**Schlumberger** (2006). Highlighting heavy oil review. https://www.slb.com/resources/publications/industry_articles/oilfield_review/2006/or2006sum03_highlighting_heavyoil.aspx

**Semenov, N.** (1935). Chemical kinetics and chain reactions, Oxford.

**Stormy, A**. (2013). A Practical introduction to programming and problem solving.

ISBN -13: 978 – 0124058767. Third Edition.

**Vyazovkin, S.** (1997). Modification of the integral Isoconversional method to account for variation in the activation energy.

*Journal of Computational Chemistry*, 22 (2). 393 – 402.

**Weijdema, J.** (1968). Determination of the oxidation kinetics of the in-situ combustion process. Report from *Koninklijke/Shell*. Exploratie producktic laboratory, Rijswijk, The Nederland.

**CURRICULUM VITAE**

**Name - Surname** : EVANS ANTO – DARKWAH

**Date of Birth and Place** : April 3rd, 1985. NKAWIE – ASHANTI, GHANA.

**E-mail** : aandarke@ymail.com

**EDUCATION** :

- **Undergraduate** : 2009, Kwame Nkrumah Univ. Of Science And Technology (KNUST), Faculty of Science, Chemistry Kumasi – Ghana.

**Professional Experience and Awards:**

- 1997 – 2000, Ghana Government Scholarships (Junior High Division).
- 2009 - 2010, Chemistry Tutor, Nkawie Senior High School.
- 2012 - 2015, Ghana/Turkish Governments scholarship award (Masters).